https://doi.org/10.5194/egusphere-2025-4368
Preprint. Discussion started: 8 October 2025

Exploring groundwater-surface water interactions and recharge in fractured mountain systems: an integrated approach

Sofia Ortenzi[1], Lucio Di Matteo[1], Daniela Valigi[1], Marco Donnini[2], Marco Dionigi[2], Davide Fronzi[3], Josie Geris[4], Fabio Guadagnano[1], Ivan Marchesini[2], Paolo Filippucci[2], Francesco Avanzi[5], Daniele Penna[2,6,7], Christian Massari[2]

[1] Department of Physics and Geology, University of Perugia, Perugia, 06123, Italy
[2] National Research Council, Research Institute for Geo-Hydrological Protection, Perugia, 06126, Italy
[3] Department of Science and Matter Engineering, Environment, and Urban Planning, Marche Polytechnic University, Ancona, 60131, Italy
[4] School of Geosciences, University of Aberdeen, Aberdeen, AB24 3UE, UK
[5] CIMA Research Foundation, University Campus of Savona, Savona, 17100, Italy
[6] Department of Agriculture, Food, Environment and Forestry, University of Florence, Firenze, 50145, Italy
[7] Forest Engineering Resources and Management Department, Oregon State University, Corvallis, OR 97331, USA

Correspondence to: Lucio Di Matteo (lucio.dimatteo@unipg.it)

Abstract. This study presents an integrated approach to map groundwater-surface water (GW-SW) interactions in a scarcely anthropized Mediterranean mountain catchment (Ussita) characterized by fractured limestone rocks with complex spatial-temporal patterns of hydrological processes. Understanding GW contributions to streams like the Ussita is crucial for addressing environmental challenges, including water resources management and evaluating ecological flows to protect aquatic ecosystems. The use of traditional hydrological techniques, such as discharge measurements along various stream stretches, combined with hydrochemical-isotopic analyses and innovative thermal drone investigations, allowed us to quantify the specific contributions of different limestone aquifers in sustaining streamflow. Integrating satellite-based meteorological datasets with in-situ observations further helped to constrain the water budget and assess the extent of the recharge area. Hydrogeochemical data analyses also revealed that the contribution of snow melt to aquifer recharge is about 20%, which is an important issue to consider for GW availability in case of future spatial-temporal changes in snow patterns. These findings can support further studies in other catchments by guiding and optimizing field campaigns to identify site-specific conditions responsible for GW inflow, from the point source to the stream stretch. Moreover, the results can help optimize resource management, mitigate climate-related risks, and support the long-term sustainability of both upstream and downstream socio-ecological systems.

1 Introduction

Carbonate aquifers in mountainous regions host strategic groundwater (GW) resources that interact dynamically with surface water (SW), influencing the quantity and quality of downstream water bodies. In such systems, baseflow—the portion of

https://doi.org/10.5194/egusphere-2025-4368
Preprint. Discussion started: 8 October 2025

streamflow derived from GW seeping into streambeds—is a key component of discharge, especially during no-recharge periods, such as prolonged droughts or seasonal dry spells typical of the Mediterranean Region (Winter, 2007; Duncan, 2019). According to a recent report by the Italian Institute of Statistics (ISTAT, 2025; https://www.istat.it/wp-content/uploads/2025/03/Report-Statistiche-sullacqua_Anni-2020-2024.pdf), the drinking water supply of about 9 million people in Central Italy comes from groundwater resources, with a substantial amount coming directly from springs (72%), followed by pumping wells (26%). Given the complexity of GW-SW interactions, water resources management typically requires treating GW and SW as a single, integrated resource, even though variations in GW storage strongly influence stream discharge (Scanlon et al., 2023), water temperature (White et al., 2023), and water quality (Conant Jr et al., 2019). Understanding GW contributions to streams is therefore essential for managing environmental water resources challenges, which also include specifying ecological flows for preserving aquatic ecosystems (Acreman and Dunbar, 2004; Lorenzoni et al., 2018; Fernández-Martínez et al., 2023). Furthermore, characterizing GW contributions supports the comprehension of processes regulating rocks' physical and chemical weathering, a key process of the global carbon cycle, both in the long- and the short-term (see e.g. Kump et al., 2000; Tipper et al., 2006; Hartmann et al., 2009; Hilton and West, 2020).

As reported by Muñoz et al. (2024), despite their importance, the understanding of mountain aquifers that ultimately sustains streamflow GW contributions remains limited (Somers and McKenzie, 2020) and understudied due to a wide range of uncertainties related to scarce information and the high cost of reliable data acquisition (Somers and McKenzie, 2020; Adler et al., 2023). Regional variations in climate, snowpack, and catchment characteristics further complicate generalizations of GW-SW interactions in mountain regions of the Mediterranean, where several geological interplaying factors, including fracturing and karst features, increase the complexity of GW systems and therefore their management (e.g., Preziosi et al., 2007; Cambi et al., 2010; Boni et al., 2010; Di Matteo et al., 2020; Lancia et al., 2020; Preziosi et al., 2022; Azimi et al., 2023; Xanke et al., 2024).

Many mountainous hydrogeological systems are increasingly stressed by overexploitation and climate change, as evidenced by GRACE satellite anomalies and in situ observations (Rateb et al., 2020). However, according to Yin et al. (2022), the applications of GRACE on local scales, despite attempts to improve the resolution of water storage estimates by integrating simulated water storage from hydrological models (data assimilation, DA), typically provide underestimated depletion signals in mountain areas. According to Dettinger (2014), expanding mountain-based networks of meteorological and streamflow observations is essential for water managers, especially when considering the impacts of uncertain future climate changes. However, collecting accurate streamflow and hydrometeorological data in mountainous terrain is logistically difficult and costly (Shakti and Sawazaki, 2021), making it challenging to understand where aquifer-stream interactions or GW outflows towards neighbouring systems occur, the latter complicated by fault zones and karst features, which strongly govern GW circulation in mountain aquifer systems (e.g., Ofterdinger et al., 2019). According to Polo et al. (2020), a special focus on Mediterranean mountain catchments is necessary to investigate the complexity of the spatial-temporal patterns of hydrological signatures. This is a key point that requires the collection of data to develop reliable water budgets and acquire hydrogeological aquifer properties (Bonacci, 1993; Dragoni et al., 2013; Di Matteo et al., 2017, 2020; Valigi et al., 2021). Closing the water

https://doi.org/10.5194/egusphere-2025-4368
Preprint. Discussion started: 8 October 2025

budget in mountainous catchments remains one of the most persistent challenges due to data demands and scale-dependent uncertainties (Levin et al., 2023; Marti et al., 2023). Recently, Zheng et al. (2025) highlighted that the non-closure of the water budget shows clear scale-dependent behaviour and is strongly influenced by hydro-meteorological conditions. In particular, the underestimation of cold-season precipitation (including snow melt) and warm-season evapotranspiration often leads to an under- or overestimation of the available recharge. Few studies investigated and quantified the role of snow melting on aquifer recharge in Mediterranean catchments (Fayad et al., 2017) and specifically for the Apennine Region (Lorenzi et al., 2023; Di Giovanni and Rusi, 2024). Currently, it is challenging to achieve water budget closure based solely on satellite-based data (e.g., Gao et al., 2010; Lv et al., 2017), underscoring the need to collect data at experimental sites in the Mediterranean region. To address persistent uncertainties in the water budget and GW-SW interactions in mountainous carbonate catchments, this study focuses on the following open research problems:

a. How does an integrated approach improve estimates of groundwater inflow to streams compared to stream-gauge data alone, helping to effectively close the water budget and reduce the error in quantifying the recharge area extension?

b. Which proportion of snow accumulation and melting affects the aquifer recharge in Central Apennine carbonate catchments?

The present study aims to answer these open questions by presenting an integrated multidisciplinary approach. It considers a mountain catchment located in the Apennine Ridge of Central Italy. Specifically, the research focuses on the Ussita stream catchment (44 km^2), which is a valuable study area in the Mediterranean Region because it is minimally affected by human activities, such as GW withdrawals or stream diversions to other catchments. In detail, the operations of a small hydropower station in the middle to high part of the catchment produce negligible effects on stream discharge, which occurs occasionally for a few hours during the week. Spot measurements, thermal drone surveys, GW and SW tracer tests, and geochemical and isotopic water sampling complement a continuous stream discharge monitoring system, making Ussita an experimental catchment to study the natural hydrological processes governing GW and their interactions with surface water, and to evaluate the contribution of baseflow along the stream reach.

Although developed for the Ussita catchment, the methodology is designed to be adaptable to other Mediterranean mountain catchments and worldwide fractured systems with limited high-elevation monitoring. This aids in achieving a comprehensive understanding of mountain hydrological systems, optimizing resource management, mitigating climate-related risks, and supporting the long-term sustainability of both upstream and downstream socio-ecological systems.

2 Materials and methods

2.1 The Ussita experimental catchment

The Ussita catchment is situated along the Apennine ridge of Central Italy and is characterized by carbonate multilayer formations belonging to the Umbria-Marche stratigraphic sequence. Figure 1a shows the geological map of the study area with the location of two nested study catchments. The catchment outlet at Madonna dell'Uccelletto (MDU) drains an area of 44

https://doi.org/10.5194/egusphere-2025-4368
Preprint. Discussion started: 8 October 2025

km^2 (S5 in Fig. 1b), whereas the stream in the upper part at Ussita Village (UV) drains 18 km^2 (S2 in Fig. 1b). The mean altitude of MDU is about 1315 m a.s.l., while the maximum and minimum altitudes are about 2256 m and 645 m a.s.l., respectively. The carbonate sequence lies on Upper Triassic evaporitic rocks, primarily composed of low-permeability anhydrites and dolomites (Evaporites Complex, EC). However, these units are not exposed in the area under investigation. Owing to the presence of shallow-water carbonate deposits and pelagic formations, the Ussita catchment is characterized by hydrogeological complexes with a range of different relative permeabilities (right-hand column in Fig. 1a, based on Pierantoni et al., 2013). More specifically, there are two high relative permeability complexes, which include the Basal Limestones Complex (BLC, composed of Calcare Massiccio and Corniola formations) and the Maiolica Complex (MAC). They host important aquifers due to strong fracturing and karstification (for BLC). BLC and MAC are separated by the Calcareous Siliceous Marly Complex (CSMC), which has relatively low permeability and is composed of formations deposited in a structural low (Rosso Ammonitico, Marne del Serrone, Calcari a Posidonia, and Calcari Diasprigni formations) and in a structural high (Bugarone). The latter outcrops in a small tectonic window in the lowest part of the MDU catchment, close to the Madonna dell'Uccelletto spring (I2 in Fig. 1b).

Above the MAC lies the Marne a Fucoidi Complex (MFC), a marly deposit of low-permeability rocks. Subsequently, marly-limestone units display moderate permeability and include the Scaglia Rossa and Scaglia Bianca formations (Scaglia Calcarea Complex, SCC). These are overlain by the Scaglia Variegata and Scaglia Cinerea formations, composed of marls and marly limestones, which also have low permeability and are grouped as the Calcareous Marly Complex (CMC), outcropping outside the MDU catchment. In the eastern part of the study area, Miocene-aged marly units (Schlier and Bisciaro) and the siliciclastic Laga Formation are predominant. These formations are part of the Terrigenous Units Complex (TUC) and typically exhibit moderate to low permeability.

Multiple tectonic events beginning in the Jurassic influenced all the formations described above, involving both extensional and compressive phases. Concerning the compression structures (Miocene-Pliocene), a key feature is the Pizzo Tre Vescovi Thrust (PTV), located in the eastern part of the study area (Fig. 1a). A system of NNW–SSE trending normal faults that developed from the Late Pliocene Quaternary extensional tectonic phase intersected later compressive structures. These faults are still active, contributing to the seismicity of the area, the latter of which occurred on October 30th, 2016 (Mw 6.5), about 15 km south of Ussita Village, triggered by the rupture of different segments of the Vettore Mt.–Bove Mt. Fault system, VBF (e.g., Brozzetti et al., 20199). This seismic sequence deeply affected the hydrogeological properties of aquifers in the headwaters of the Nera River, into which the Ussita stream flows (Fig. 1), by different transient co-seismic effects such as the release of crustal fluids following elastic co-seismic deformations, the increase in water pressure following the rise in the hydraulic gradient in the aquifer, and the changes in rock permeability due to microcracks, unblocking of pre-existing fractures, and fracture cleaning (Petitta et al., 2018; Di Matteo et al., 2020; Mastrorillo et al., 2020; Di Matteo et al., 2021; Cambi et al., 2022; Mastrorillo et al., 2023). However, according to Di Matteo et al. (2021), starting in 2019, the pre-seismic conditions have now recovered, and the total river flow can be analyzed in the context of the meteo-climatic processes regulating the GW-SW interactions.

https://doi.org/10.5194/egusphere-2025-4368
Preprint. Discussion started: 8 October 2025

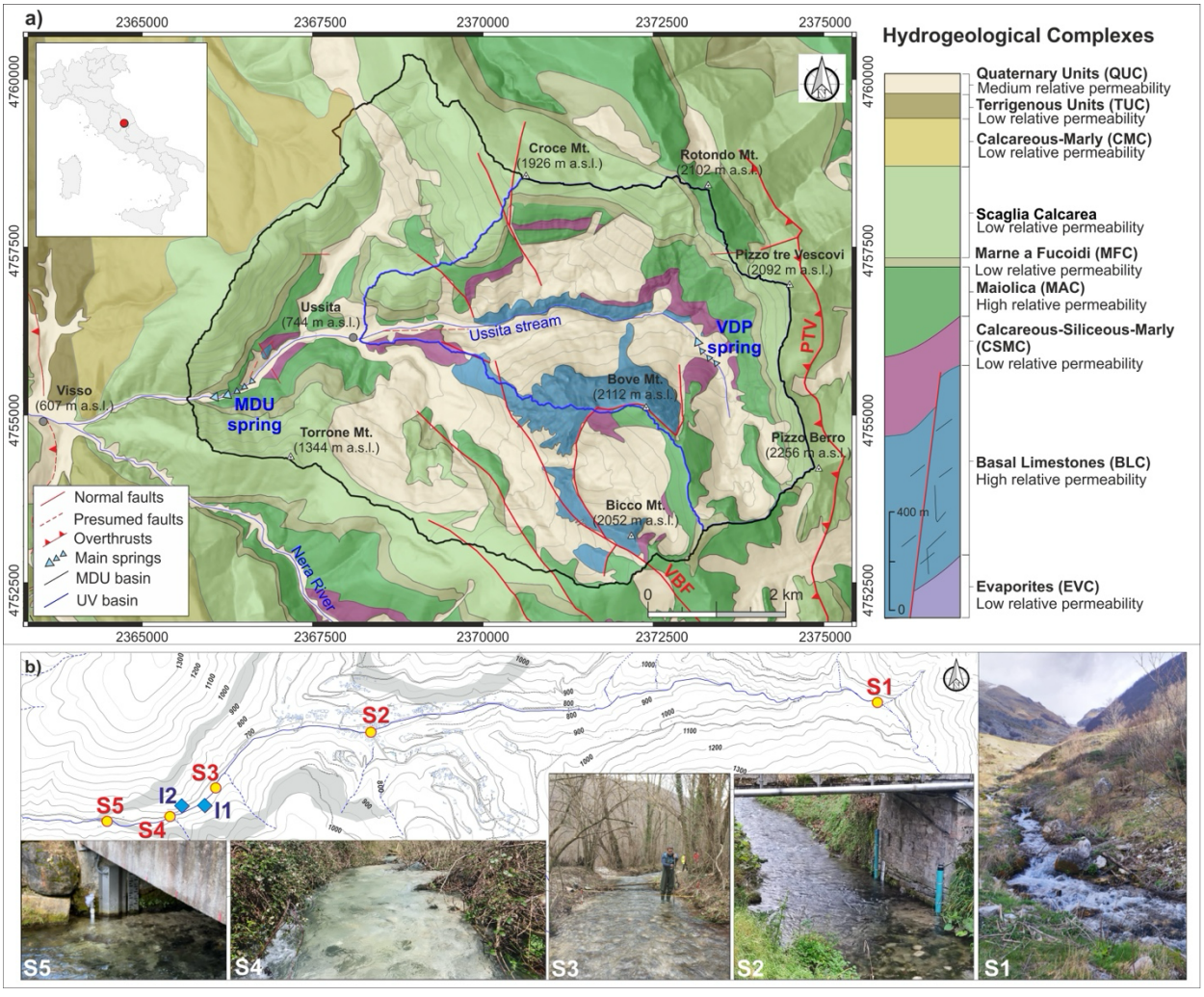

135 **Figure 1: a) Map of hydrogeological complexes of the Ussita Stream catchment based on the geological map of Pierantoni et al. (2013). MDU = Ussita catchment at Madonna Dell'Uccelletto (MDU); UV = Ussita catchment at Ussita Village (UV); VDP = Val Di Panico spring; VBF = Mt. Vettore-Mt. Bove Fault system; PTV = Pizzo Tre Vescovi thrust. b) The location of stream gauges with reliable rating curves (S2 and S5), stream sections monitored by spot measurements with the OTT MF Pro flow meter (S1, S3, and S4), and GW inflow (I1 and I2). The grey shadow zone represents the outcropping of the low-permeability Marne a Fucoidi Complex**
140 **(MFC).**

2.2 Monitoring network

2.2.1 Ground-based hydrometeorological monitoring network

Daily stream levels of the Ussita stream were collected at the outlet of the two sub catchments investigated, S2 and S5, placed at the closure of the UV and MDU catchments, respectively (Fig. 1b). In detail, stream level data of the S5 section were

https://doi.org/10.5194/egusphere-2025-4368
Preprint. Discussion started: 8 October 2025

collected from the SIRMIP online monitoring network (Civil Protection Agency of Marche Region, Central Italy). At the same time, those of S2 were made available thanks to the hydrological monitoring infrastructure available at the Sibillini National Park Critical Zone observatory (SINCZONE, https://cnr-eco-hydrology-lab.org/sinczone-observatory), developed and managed by CNR-IRPI (Istituto di Ricerca per la Protezione Idrogeologica of CNR). Overall, the observation period for S5 was from 2019 to 2024, and for S2, this was from 2022 to 2024.

Rating curves of both stream gauges were obtained from spot measurements with the OTT MF Pro flow meter (ten measurements in the flow range 0.70-1.18 m^3/s) carried out during the 2022-2025 period: these rating curves have been used to convert stream levels (H) into stream discharge data (Q). Moreover, during the same period, the spot discharge measurements by the OTT MF Pro flow were extended to stream sections S1, S3, S4, and S5 (Fig. 1b) to investigate GW inflow from limestone aquifers across the larger stream stretch.

The experimental setup included six ground-based weather stations (Table S1 and Fig. 2). The Ussita and Casali stations measured temperature and rainfall data at hourly intervals inside the catchment, which were also aggregated to different timescales (hourly, daily, monthly, and yearly). As reported in Table S1, the Ussita station has the longest dataset, and it has been used as a reference to characterize the mean precipitation over the Ussita catchment. As reported by Di Matteo et al. (2021) and Gentilucci et al. (2021), a substantial underestimation of precipitation for the Monte Bove Sud rain gauge has been highlighted compared to those placed at lower elevations. Ussita, ENDESA, and Ponte Tavola rain gauges are used for this analysis, allowing us to demonstrate the unreliability of stations at high altitudes and exclude them from the computation of the precipitation over the catchment.

Snow depth was measured at two stations (Monte Bove Sud and Pizzo Tre Vescovi, see Fig. 2). However, in the investigation period, they show substantial data gaps, which make them unsuitable for the analysis. It is a common issue in the mountain regions of the Italian Apennines and Alps, where the presence of precipitation and snow depth monitoring stations at higher elevations is scarce or not representative of the mean altitude of mountain catchments (Cambi et al., 2010; Daly et al., 2017; Ly et al., 2013; Di Matteo et al., 2017; Avanzi et al., 2024; Girotto et al., 2024). Whereas the role of snow melt cannot be neglected in the highest elevation areas of Mediterranean catchments, which receive most of the winter/spring precipitation as snow, this is of less concern for the mid-elevation areas, which have a mixed precipitation regime (e.g., Fayad et al., 2017).

https://doi.org/10.5194/egusphere-2025-4368
Preprint. Discussion started: 8 October 2025

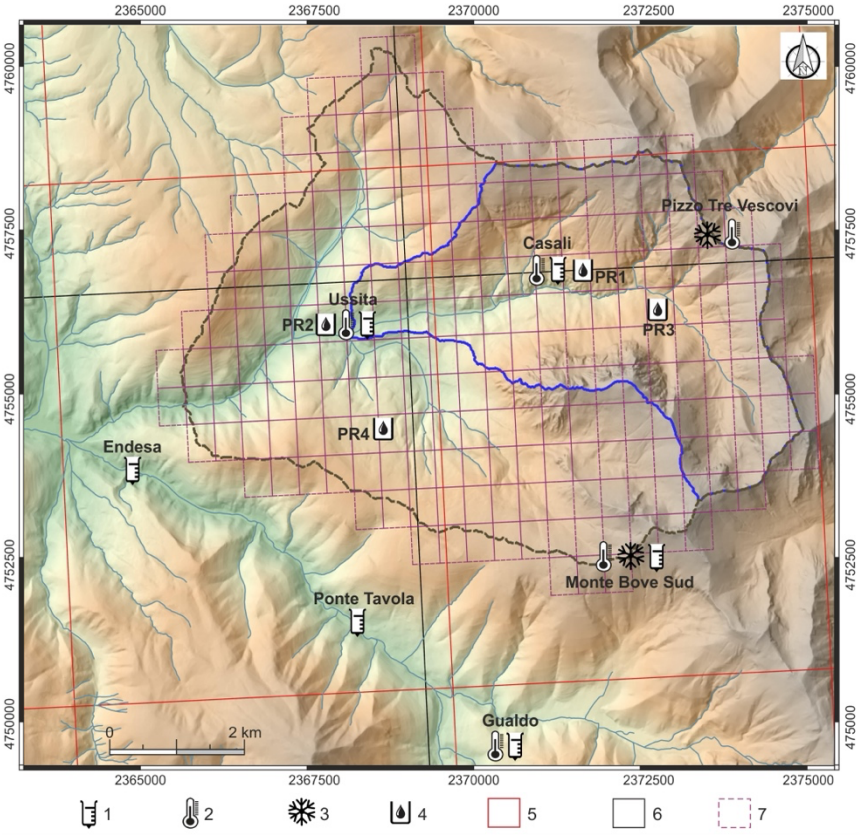

Figure 2: The location of thermo-pluviometric and snow depth gauges with rain water samples for isotopic analyses and dataset product grids. 1 – rainfall; 2 – air temperature; 3 – snow depth; 4 – isotopic rain collectors; 5 – MERIDA grid; 6 – ERA5-Land and IMERG grid; 7 – IT-SNOW grid.

2.2.2 Precipitation data from regional and global datasets

To overcome the problem of data scarcity, complementary precipitation products were used to allow for the estimation of rainfall (P_{rain}) and snow melt (P_{snow}) at different spatial-temporal resolutions over the MDU catchment. Different independent sources were used to consider uncertainty in the estimates from the products and their impact on the results.

2.2.2.1 Integrated Multi-satellitE Retrievals for Global Precipitation Measurements (GPM IMERG)

The GPM IMERG algorithm (Huffman et al., 2023). intercalibrates, merges, and interpolates the precipitation estimates from GPM satellites, providing a half-hourly rainfall product (merged also into monthly and daily) with a spatial resolution of 0.1°x0.1° (about 10 km, Fig. 2). The system is run three times, providing "Early," "Late," and "Final" rainfall estimates. The "Final" product is calibrated with monthly data from rain gauges and is released about four months after the observation month.

https://doi.org/10.5194/egusphere-2025-4368
Preprint. Discussion started: 8 October 2025

2.2.2.2 European Reanalysis 5th generation (ERA5-Land)

ERA5-Land (Muñoz Sabater, 2019; C3S, 2022) is a state-of-the-art dataset released by the European Centre for Medium-Range Weather Forecasts (ECMWF). It offers high-resolution (about 9 km, Fig. 2) global data at different time steps, providing detailed information on land surface variables, including precipitation (REF).

2.2.2.3 The Meteorological Reanalysis Italian Dataset (MERIDA)

MERIDA (Bonanno et al., 2019) is a more regionally focused reanalysis product (resolution of about 7 km, Fig. 2). It consists of dynamically downscaling the ERA5 global reanalysis fields using the Weather Research and Forecasting (WRF-ARW) mesoscale model (Skamarock et al., 2008). As reported in Bonanno et al. (2019), the robustness of MERIDA is guaranteed by the assimilation of the surface-based (SYNOP) data (WMO, 2014) and the application of the Optimal Interpolation (OI) technique (e.g., Uboldi et al., 2008) on the 2 m temperature and precipitation fields simulated by WRF.

2.2.2.4 The Modified Conditional Merging (MCM) algorithm

The MCM algorithm (Pignone et al., 2015) generates precipitation estimates by blending data from this national rain-gauge and radar networks. After defining the spatiotemporal domain of interest, rainfall data from each rain gauge are interpolated using the GRISO method (random generator of spatial interpolation from uncertain observations; Pignone et al., 2010). The same procedure was performed on radar data. The precipitation data are sampled on rain gauge locations using the interpolation radar data map, and the same GRISO parameters are adopted to interpolate rain gauge data (e.g., Loglisci et al., 2024). Afterwards, precipitation data from the original radar map and the GRISO interpolation on radar data are compared. Finally, the sum of the difference map and the rain gauge interpolation provides the MCM map.

2.2.2.5 IT-SNOW product

Snow Water Equivalent (SWE) data were derived from the IT-SNOW product (Avanzi et al., 2023) developed by CIMA Research Foundation for the Italian Civil Protection Department. IT-SNOW is a snow reanalysis for Italy, blending modeling, in situ data, and satellite observations, with a spatial resolution of about 500 m (Fig. 2). It is a snow reanalysis providing estimates of snow patterns in topographically and climatically complex regions across Italy (Avanzi et al., 2023). The dataset (IT-SNOW v4.0) includes daily reanalyzed outputs of Snow Water Equivalent (SWE), snow depth, density, and bulk liquid water content from S3M Italy for water years 2010 through 2024 (the dataset is freely available at https://zenodo.org/records/14093436).

https://doi.org/10.5194/egusphere-2025-4368
Preprint. Discussion started: 8 October 2025

The SWE data from the IT-SNOW dataset were used to extract and analyze the contribution of snow melt at a monthly scale (P_{snow}) over the MDU catchment. The analysis was carried out following the workflow in Fig. 3. In detail, when SWE was zero (no snow), the rainfall (if present) was the only input to the system (P_{rain}). When snow cover was present, a day-by-day and cell-by-cell evaluation was made to check for a change in SWE compared to the previous day (ΔSWE). In the case of ΔSWE<0, it was assumed that snow melt occurred, contributing to the P_{snow}.

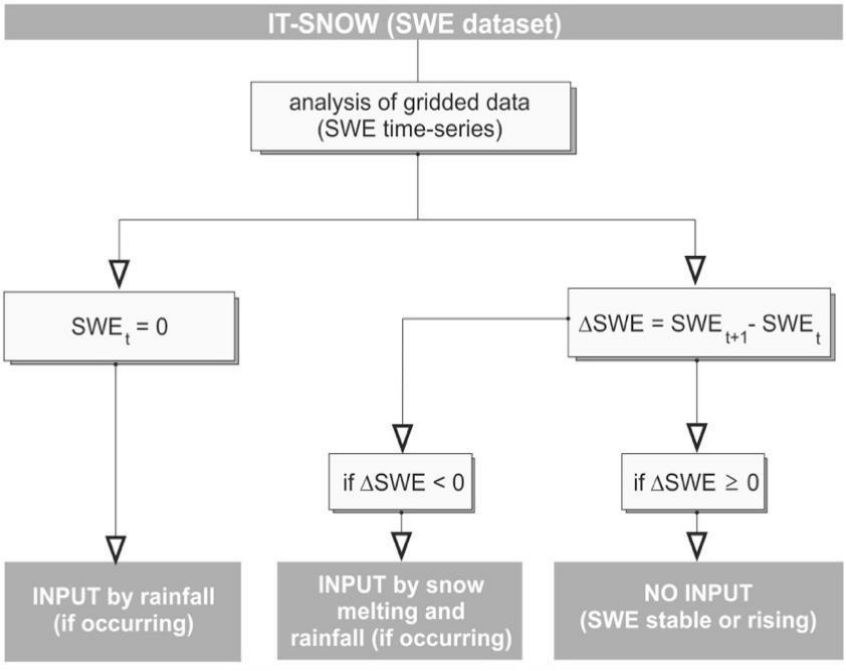

Figure 3: Workflow for analyzing water availability contribution from IT-SNOW's SWE data.

2.3 Stream tracer tests

Discharge measurements were complemented with the instantaneous release of an artificial tracer (i.e., Sodium fluorescein, Na-Fluorescein, analytical formula $C_{20}H_{10}Na_2O_5$). Tracer-based measurement was performed in January 2024 concurrently with the OTT MF Pro to allow cross-validation of the results. The mass (m) of Na-Fluorescein injected into the stream ranged from 0.7 g (at S3) to 1.9 g (at S5), with the tracer released approximately 200 meters upstream of the measurement sections to ensure adequate mixing and homogeneous dispersion in the streamflow. Tracer passage at the monitored sections was tracked using a PME fluorometric probe (Cyclops-7 Logger, measurement range 0-150 µg/L, and resolution: 0.01 µg/L), which was previously calibrated with standard solutions of 0 µg/L (stream water) and 100 µg/L. Tracer concentration data were recorded at 5-second intervals and expressed as concentration over time as a breakthrough curve (BTC).

Discharge (Q) was subsequently calculated by integrating the BTC over time, following Equation 1:

$$Q = \frac{m}{\int_{t_0}^{t_f} c\, dt} \quad (1)$$

https://doi.org/10.5194/egusphere-2025-4368
Preprint. Discussion started: 8 October 2025

Where:

m = injected mass.

c = tracer concentration over time (dt).

t_o = starting period of the discharge measurement.

t_f = ending period of the discharge measurement.

Most of the discharge measurements were carried out in the lower part of the MDU catchment (Fig. 1b), where GW inflow was detected in previous studies up to the no-flow boundary of MFC (Tarragoni, 2006; Di Domenicantonio et al., 2009; Mastrorillo et al., 2009; Boni et al., 2010; Di Matteo et al., 2020; Nanni et al., 2020). In such a hydrogeological framework, the location of the S5 stream gauge (Fig. 1b) ensured discharge monitoring at the outlet of the hydrogeological system feeding the Ussita stream. According to Boni et al. (2010), part of the water downstream of S1 (VDP spring) was collected into a pipeline that releases the water upstream section S2 (daily, this stream diversion's effect is negligible).

2.4 Acquisition and treatment of hydrochemical and isotopic data

From November 2023 to March 2025, systematic campaigns at an approximately monthly frequency were performed to collect water samples at S1, S2, S3, I1, I2, and S5 (see Fig. 1b) for the determination of major soluble ion (Ca^{2+}, Mg^{2+}, Na^{+}, K^{+}, SO_4^{2+}, Cl^{-}, HCO_3^{-}) concentrations, as well as the isotopic composition of water (δD, $\delta^{18}O$). In the field, pH, temperature, and electrical conductivity were determined by using a multi-parameter portable meter (model XS PC 7 Vio), whilst the HCO_3^{-} concentration was determined by acidimetric titration in a sample of 250 ml, adding HCl 0.1 N with a portable dosimeter and using methyl orange as a colorimetric indicator (e.g., Donnini et al., 2016; Frondini et al., 2019; Chiodini et al., 2021; Donnini et al., 2025). Additionally, δD and $\delta^{18}O$ were determined in precipitation samples collected approximately monthly at PR1, PR2, PR3, and PR4 (see Fig. 2 for location and Table S1 for altitude details), by using funnel-and-nozzle-based precipitation samplers. The wide-mouthed funnel allows for the collection of a representative rainfall sample, while the narrow nozzle directs the rainwater into a collection bottle, thereby reducing the water's surface area exposed to the atmosphere and minimizing evaporation. To collect precipitation in the form of snow, a dark tube was placed above the funnel of the PR3 station (elevation of about 1200 m a.s.l.). This tube allowed the snow to be collected and melted before it entered in the collection bottle.

The concentration of major soluble cations and anions of stream water (Ca^{2+}, Mg^{2+}, Na^{+}, K^{+}, SO_4^{2+}, Cl^{-}) was obtained by suppressed ionic chromatography (AQUION and ICS-2100 Dionex supplied by ThermoFisher Scientific, Waltham, MA, USA). Multi-ion calibration standards were prepared from single-component standard solutions for ion chromatography (Fluka-TraceCERTTM, 1000 ± 4 ppm, Honeywell International Inc., Charlotte, NC, USA). The linearity of calibration curves was verified in the 0.5-50 ppm interval. Table S2 and Table S3 show the limit of detection and the limit of quantification.

The isotopic analyses were performed through standard mass spectrometry (PICARRO L2130-I Cavity Ring-Down Spectroscopy CRDS). The values of δD ($^2H/^1H$) and of $\delta^{18}O$ ($^{18}O/^{16}O$) are referred to as δ (‰) of the standard V-SMOW (Vienna Standard Mean Ocean Water). Analytical errors are: ±1‰ for δD, ±0.08‰ for $\delta^{18}O$.

https://doi.org/10.5194/egusphere-2025-4368
Preprint. Discussion started: 8 October 2025

The isotopic composition of precipitation samples collected at stations PR1, PR2, PR3, and PR4, together with those of Tazioli et al. (2004), collected a few kilometers south of the MDU catchment (elevation of 1800 m a.s.l.), was used to derive:

i) The Local Meteoric Water Line (LMWL).
ii) The $\delta^{18}O$–elevation relationship, to compute the Isotope Recharge Elevation (CIRE) of Ussita stream waters (e.g., S1, S2, S3, I1, I2, and S5), following the methodology of Petitta et al. (2010).

For each Ussita stream water sample, the line-conditioned excess (lc-excess) values were calculated according to the approach described by Noor et al. (2022) and references therein, using the following equation (Eq. 2):

$$\text{Ic} - \text{excess} = \delta D - a * \delta^{18}O - b \quad (2)$$

where:

a and b = the slope and intercept of the LMWL, respectively.

Negative lc-excess values indicate that the water has undergone evaporation-induced isotopic fractionation, whereas positive values suggest minimal or no evaporation (Landwehr and Coplen, 2006).

To explore the $\delta^{18}O$–elevation relationship, we applied the approach proposed by Tazioli et al. (2024). First, for each precipitation collector, the volume of water collected during each sampling period was measured manually. The average $\delta^{18}O$ value of precipitation was then determined by weighting each isotopic value according to the amount of water collected during that sampling period, relative to the total precipitation over the entire observation period. This was done using Eq. 3:

$$\delta = \frac{\sum(\delta i * Pi)}{\sum Pi} \quad (3)$$

where:

δ = weighted average of isotopes.

δi = the isotopic value of a single sample.

Pi = the corresponding precipitation amount.

Next, using the known elevations of the precipitation collectors, the $\delta^{18}O$ values were plotted against elevation to establish a linear $\delta^{18}O$–elevation relationship. This regression was then applied to the $\delta^{18}O$ values of the Ussita stream water samples to compute their respective Isotope Recharge Elevation (CIRE).

2.5 Baseflow separation

Among the available indices, the Base Flow Index (BFI) is one of the most widely used for assessing baseflow contribution to total streamflow (Nathan and McMahon, 1990; Smakhtin, 2001; Longobardi and Villani, 2023); it is the ratio between the mean annual baseflow (BF) and mean annual streamflow (Q). To compute the BFI in sections S2 and S5, the Base Flow (BF)

https://doi.org/10.5194/egusphere-2025-4368
Preprint. Discussion started: 8 October 2025

component has been separated from the stream hydrograph. As recently discussed by Nagy et al. (2024), separating stream flow into baseflow and direct runoff is a non-trivial task in hydrology since, very commonly, no observations are available for baseflow. Among the available separation techniques of streamflow (e.g., Furey and Gupta, 2001) in this study, the one-parameter recursive digital filter developed by Lyne and Hollick (1979) was used (Eq. 4), which is a simple technique providing an intuitively satisfactory representation of baseflow (e.g., Duncan, 2019). In this method, the baseflow at time t (B_t) is separated from the total stream discharge at time t (Q_t) using a filter parameter k that effectively separates low-frequency signals (associated with baseflow). Selecting an appropriate k-parameter value is an open question, even if the Lyne and Hollick (1979) method is considered helpful for comparative hydrology and regionalization, as it can be used to characterize differences between catchments consistently (Landson, 2013). According to Nathan and McMahon (1990), the Lyne and Hollick filter's application requires selecting a number of passes and a single k-parameter value. More specifically, the k-parameter affects the degree of baseflow attenuation, and the number of passes determines the degree of smoothing (Nagy et al., 2024). The k-parameter generally ranges between 0.90 and 0.99 (e.g., Kang et al., 2022). Although there is little direct link to physical catchment processes and no calibration or other subjective user inputs are required (Duncan, 2019), some authors assumed $k = e^{-\alpha t}$ (Chapman, 1991; Tan et al., 2009), where α is the recession coefficient estimated by the Master Recession Curve (MRC) considering daily or hourly discharge time steps (e.g., Tallaksen, 1995; Posavec et al., 2006; Gregor and Malik, 2012; Di Matteo et al., 2017; Carlotto and Cheffe, 2019; Di Matteo et al., 2020). Following the approaches in Chapman (1991) and Tan et al. (2009), the k-parameter value for each catchment was estimated, and the recursive filter was applied by setting the number of passes to three (forward–backward-forward) to minimize phase distortion effects on the peak values (Nathan and McMahon, 1990).

$$B_t = kB_{(t-1)} + \frac{(1+k)}{2}(Q_t - Q_{t-1}) \quad (4)$$

2.6 Thermal drone investigations

In fluvial environments, thermal anomalies on the water surface often indicate zones where groundwater enters the stream, as groundwater typically exhibits a temperature contrast with surface water. Furthermore, the temperature of water bodies frequently differs from that of the surrounding terrain, allowing the detection of watercourses even when they are obscured by vegetation. This method, therefore, enables detailed spatial mapping of groundwater discharge areas and hidden streams, enhancing the accuracy of hydrological assessments and monitoring.

In the present study, a thermal drone analysis was conducted to investigate the location of GW inflows along about 1100 m stretch between sites S3 and S5 of the stream. A DJI MAVIC 2 ENTERPRISE Dual drone, with an integrated thermal sensor, was employed to acquire high-resolution thermal images of the stream surface under stable meteorological conditions. The camera had a resolution of 640 × 480 pixels and a pixel pitch of 12 µm. The flights were performed at 90 m height, which delivered an approximate ground resolution of ~0.12 m. The spectral response was in the range of 8–14 µm. The investigated stream stretch was divided into three smaller areas, and three different flights were conducted on January 30, 2025, to analyze

https://doi.org/10.5194/egusphere-2025-4368
Preprint. Discussion started: 8 October 2025

the whole region (take-off at 10:37, 11:02, and 11:49 local time, respectively). The percentage of the Frontal and Side Overlap ratio was fixed at 85%. The data were then processed using Agisoft Metashape Professional to post-process the data and insert the position of 6 control markers.

Water temperature was measured on-site at multiple locations to serve as a reference. These measurements were used to calibrate the average water emissivity required to convert the black-body temperature observed by the thermal camera into actual water temperature, based on the Stefan–Boltzmann equation (Eq. 5):

$$M = \sigma T_{bb}^4 = \varepsilon \sigma T^4 \quad (5)$$

where:

T = actual temperature of the water (in Kelvin).

M = total energy emitted from the surface.

ε = emissivity of water.

σ = Stefan–Boltzmann constant.

T_{bb} = black-body temperature (in Kelvin) measured by the drone.

The calibrated emissivity was found to be 0.935, which is consistent with values reported in the literature.

2.7 Water budget components and computation

The water budget is a key management tool that accounts for inflows, outflows, and changes in storage (DS) in a specific system over a specific period. The following subsections (2.7.1 and 2.7.2) detail methods to estimate the actual Evapotranspiration (ET) and the change in storage (ΔS), which, compared to other water budget components (rainfall, stream discharge, withdrawals, etc.), are generally estimated in mountain regions with empirical methods or with remote sensing. Section 2.7.3 details the approach used for the water budget computation.

2.7.1 Estimation of ET

ET values were estimated monthly and then averaged on an annual scale using different techniques relying on ground-based meteorological data and remote sensing estimations.

The Thornthwaite-Mather (1955, 1957) method has been commonly used in mountain areas of Central Italy, and ET estimations have been found to be reliable (e.g., Di Matteo et al., 2017; Mammoliti et al., 2021; Rossi et al., 2022). This method was chosen because standard climatological records of solar radiation (sunshine), air temperature, humidity, and wind speed are either unavailable for the period of analysis or contain significant data gaps. As a result, more detailed methods such as the FAO-56 Penman–Monteith equation (Allen et al., 1998) could not be applied. The monthly ET values were computed over the hydrogeological year (from October to the following September) using the WaterbaLANce WebApp based on the Thornthwaite–Mather method developed by Mammoliti et al. (2021). Since the Ussita catchment is mainly characterized by leptosol (very shallow soils over hard rocks or calcareous materials; Costantini et al., 2012,

https://doi.org/10.5194/egusphere-2025-4368
Preprint. Discussion started: 8 October 2025

https://esdac.jrc.ec.europa.eu/images/Eudasm/IT/2012Carta_Suoli_Italia.jpg) and is covered by about 90% of forests (based on the CORINE Land Cover 2018 database), the Available Water Capacity (AWC) was set to 100 mm and 150 mm (Thornthwaite-Mather, 1957).

Monthly ET data of the MOD16A2 v061 product were also used (hereafter MODIS), providing an 8-day, monthly, and annual dataset with a 500 m pixel size using a modified Penman-Monteith method from 2002 to present (Mu et al., 2011). The ET value from this remote sensing corresponds to the sum of the evaporation from the wet canopy surface (E_{Wet}), the transpiration from the dry canopy surface (T_{Dry}), and the evaporation from the soil surface (E_{Soil}) (e.g., Gallego et al., 2023).

ET data were also collected from EUMETSAT LSA SAF (Land Surface Analysis Satellite Application Facility); it provides global net evapotranspiration at a daily scale (0.5°x0.5° grid).

The estimated ET value with the above methods has been subtracted from ground-based and remote sensing P_{rain} data, obtaining the water surplus values ($S = P_{rain} - ET$), which have been compared with the Italian-scale GIS-based procedure (BIGBANG 8.0 "Nationwide GIS-Based hydrological budget on a regular grid", Braca et al., 2024). The BIGBANG 8.0 presents the S values over a 1x1 km grid, which can be downloaded from the SINAnet ISPRA website (Sistema Informativo Nazionale Ambiente of Istituto Superiore per la Protezione e Ricerca Ambientale; https://groupware.sinanet.isprambiente.it/bigbang-data/library/bigbang_80/ascii_grid). The monthly S is calculated for the 1951-2023 period by subtracting the interpolated precipitation (with Natural Neighbours 2 step) from the actual evapotranspiration (ET) computed with the Thornthwaite-Mather method.

2.7.2 Estimation of the water storage changes (ΔS)

The water storage changes (ΔS) must be considered in the hydrogeological analysis since the water budget is carried out over four years (2019-2023 period), which does not allow this component to be neglected a priori. As for other mountain systems, piezometric observations were unavailable for computing the ΔS; thus, we used the approach proposed by Korkmaz (1990) based on stream recession analysis. In detail, for stream discharge described by the Maillet exponential relationship (as for the Ussita stream, e.g., Di Matteo et al., 2020), it is possible to calculate the recession coefficient values (α) for each year (i). For example, considering the period from October to the following September, which includes two consecutive years (i and i+1), it is possible to compute the storage variation (ΔS) for each hydrological year using Eq. 6.

$$\Delta S = V_m - V_0 = 86400 * \left(\frac{Q_m}{\alpha_{i+1}} - \frac{Q_0}{\alpha_i}\right) \quad (6)$$

Where:

ΔS = dynamic reserve change during the hydrological year.

Q_m and V_m = streamflow and dynamic reserve at the end of the period.

Q_0 and V_0 = streamflow and dynamic reserve at the beginning of the period.

α_m and α_0 = recession coefficient for years i and i+1.

2.7.3 Water budget computation

https://doi.org/10.5194/egusphere-2025-4368
Preprint. Discussion started: 8 October 2025

Equations 7 and 8 mathematically express the water budget for a small catchment not affected by withdrawals or stream diversions towards other systems (Healy et al., 2007), as occurs for the MDU catchment. Each water budget term can be expressed as depth per unit time or volume per unit time (Mitsch and Gosselink, 2000).

$$P + Q_{in}^{gw} = ET + (Q + Q_{out}^{gw}) + \Delta S \quad (7)$$

$$P - ET = WS = Q + (Q_{out}^{gw} - Q_{in}^{gw}) + \Delta S \quad (8)$$

Where:

P = total precipitation.

Q_{in}^{gw} = groundwater inflow into the catchment.

ET = actual evapotranspiration.

Q = total streamflow at the closure of the catchment (surface runoff plus base flow).

WS = water surplus.

Q_{out}^{gw} = groundwater outflow towards neighboring hydrogeological systems.

ΔS = change in water storage.

The water outflow from the catchment ($Q+Q_{out}^{gw}$, in Eq. 7) represents the integrated response to all hydrogeological processes within the catchment (e.g., Singh and Woolhiser, 2002; Kirchner, 2009). According to Schaller and Fan (2009), under the assumption of no ΔS changes, a simple indicator of the partition of the water surplus (WS) is the Q/WS ratio. A Q/WS < 1 indicates that a portion of WS failed to emerge as stream outflow (i.e., the catchment drains water towards other systems, acting as a "groundwater exporter"). On the contrary, if Q/WS > 1, the observed stream discharge must include groundwater inflow from the neighboring systems (i.e., the catchment must be a "groundwater importer"). Scanlon et al. (2002) proposed an expanded form of the water budget (Eq. 9) that considers the two precipitation components, P_{rain} (liquid precipitation) and P_{snow} (snow melt).

$$P_{rain} + P_{snow} + Q_{in}^{gw} = ET + (Q + Q_{out}^{gw}) + \Delta S \quad (9)$$

Equation 9 can be rewritten as follows (Eq. 10).

$$(Q_{in}^{gw} - Q_{out}^{gw}) = -(P_{rain} - ET) - P_{snow} + Q + \Delta S = -(WS + P_{snow}) + Q + \Delta S \quad (10)$$

In Eq. 10, the water budget's only unknown component is $(Q_{in}^{gw} - Q_{out}^{gw})$, while the others can be measured (e.g., Q) or estimated (P_{rain}, P_{snow}, ET, and ΔS). According to Viaroli et al. (2018), quantifying groundwater exchanges in mountain regions is challenging since the system's boundary conditions are not well-defined. The geological-structural complexity of the Apennine chain (which includes the study area of this work) complicates the accurate assessment of groundwater inflows and outflows (Filippini et al., 2015). These hidden water budget components may constitute a considerable portion of groundwater

https://doi.org/10.5194/egusphere-2025-4368
Preprint. Discussion started: 8 October 2025

availability (Carrillo Rivera, 2000). Regardless, the unknown component of Eq. 10 ($Q_{in}^{gw} - Q_{out}^{gw}$) can be computed by introducing the measured and/or estimated components of the right side of Eq. 10. Considering the catchment area A as system, a value of $Q_{in}^{gw} - Q_{out}^{gw} >> 0$ means that, net of uncertainties in the estimation of the water budget components, there is a groundwater inflow (i.e., the hydrogeological basin A* is much larger than the catchment area A). Figure 4 shows a schematic hydrogeological system with groundwater inflow into the catchment (A*≫A).

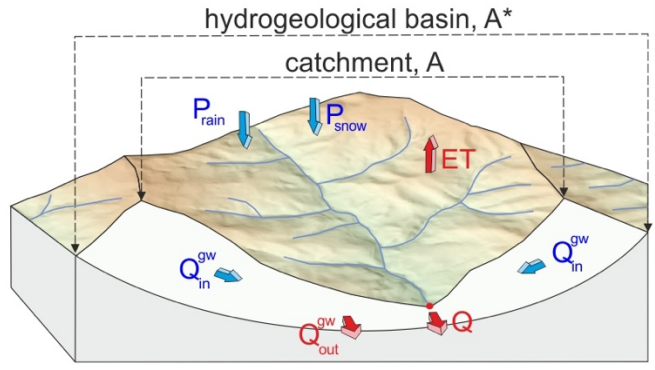

Figure 4: Schematic representation of a hydrogeological system with groundwater inflow coming outside the catchment area (A). A* = recharge area.

After computing $Q_{in}^{gw} - Q_{out}^{gw}$, it is possible to obtain the recharge area (A*) by applying Eq. 11.

$$A^* = A + \frac{(Q_{in}^{gw} - Q_{out}^{gw})}{(WS + P_{snow})} * A \quad (11)$$

To evaluate the recharge area extent, two water budget experiments are considered by combining the different available datasets for computing WS and P_{snow}. In detail, the following experiments are carried out:

- Case I, considering only the WS as input in Equation 11.
- Case II, considering both WS and P_{snow} as input in Equation 11.

For Case I, the WS values are computed as follows:

- Two estimations with the Thornthwaite–Mather method (T-M) using ground-based monthly rainfall and temperature data from the Ussita weather station and considering the Field Capacity (FC) of 100 mm and 150 mm, according to the land use and soil characteristics.
- One estimation with the BIGBANG data (in this case, the S values have been downloaded from the SINAnet ISPRA).
- Eight estimations were made by subtracting the gridded rainfall estimates (MCM, ERA5, MERIDA, and IMERG) from the gridded ET values by MODIS and LSA SAF estimations.

For Case II, the WS values computed as for Case I were summed monthly to the P_{snow} values derived from SWE of IT-SNOW, following the procedure in Fig. 3.

https://doi.org/10.5194/egusphere-2025-4368
Preprint. Discussion started: 8 October 2025

3 Results

3.1 GW-SW interactions along the stream

The integrated monitoring network of the Ussita catchment facilitated the understanding of factors influencing GW-SW interactions at multiple scales. Figure 5a displays the continuous discharge data collected at stream gauges S2 and S5 (Fig. 1b), along with spot measurements taken by OTT MF Pro at sections S1, S3, S4, and S5.

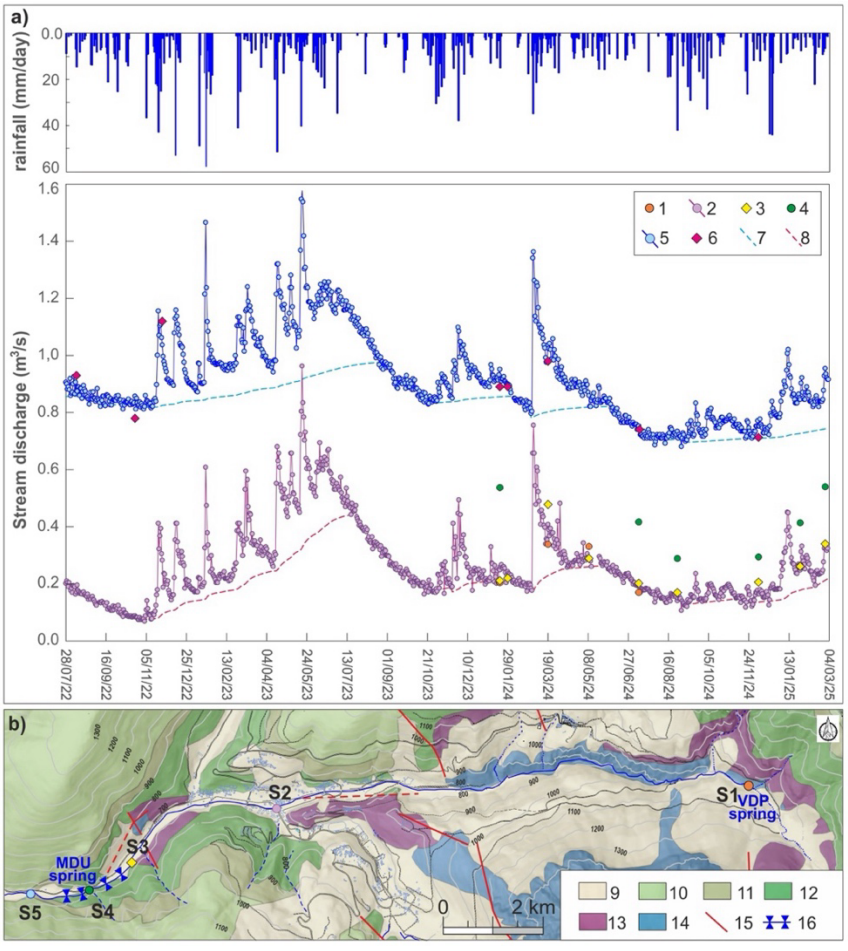

Figure 5: a) Daily stream discharge data at stream gauges S2 and S5 with rainfalls recorded at Ussita gauge and base flow curves and the discrete monitoring carried out along the stream (1 – S1 section; 2 – S2 section; 3 – S3 section; 4 – S4 section; 5 – S5 section; 6 – discrete monitoring in S5 section; 7 – Base Flow at S5 section; 8 – Base Flow at S2 section). b) location of stream sections on the geological map of Fig. 1a (9 – QUC; 10 – SCC; 11 – MFC; 12 – MAC; 13 – CSMC; 14 – BLC; 15 – Normal faults; 16 – Main GW inflows to the stream).

Moving from S1 to S3 (see Fig. 5b for the location of stream sections), the stream discharge during the no-recharge periods (e.g., stream discharge values are equal to baseflow) remains almost stable, indicating that the stream is mainly sustained by

https://doi.org/10.5194/egusphere-2025-4368
Preprint. Discussion started: 8 October 2025

the VDP spring; thus, no significant GW inflows are present downstream of the spring up to section S3. It should be noted that downstream of S3 towards S5, no tributaries that feed the Ussita stream are present. Based on mean discharge data from spot OTT MF Pro measurements acquired during the no-recharge periods (2022-2024), an initial increase in stream discharge due to GW inflow was registered between S3 and S4, estimated at 200 L/s. Downstream of S4, during 2022-2024, a further mean discharge increase of 450 L/s was measured up to the closing section of the MDU catchment (section S5). Overall, between sections S3 and S5, a mean discharge increase of about 650 L/s is recorded. This evaluation was also confirmed by the discharge measurements conducted by tracer injection on January 29, 2024 (Fig. S1), at the beginning of a stream recession phase (Fig. 5a). Between S3 and S5, a stream discharge increase of about 695 L/s was registered, a value close to the OTT MF Pro measurements (660 L/s) carried out during the tracer test, confirming the reliability of the streamflow measurement system. Figure 5a also shows the base flow (BF) curves estimated for the S2 and S5 stream sections. According to Chapman (1991) and Tan et al. (2009), the filter parameter k was estimated by the recession constant derived from the MRC. The stream discharge data in the recession periods for both S2 and S5 sections are fitted by the Maillet (1905) recession model, giving α values of -0.0100 day^{-1} and -0.0033 day^{-1}, respectively. Then the k filters were set at 0.99 for the S2 section and 0.997 for the S5 section. The analysis of BF curves allowed the calculation of the BFI value in the two stream sections: it moved from about 0.80 in S2 to 0.90 in S5, highlighting the role of GW inflow along the stream stretch (S3-S5) in sustaining the stream discharge (Fig. 5a). The drone survey carried out in January 2024 has made it possible to identify stream stretches with groundwater inflows in the stream left and right banks (difficult to locate by optical drone survey due to dense vegetation, Fig. 6a). From Figure 6b it can be seen that 1-2 °C warmer water entered the main stream channel from I1 (left bank upstream S4) and I2 (right bank downstream S4), with some other diffuse GW inflow along the stream reach surveyed.

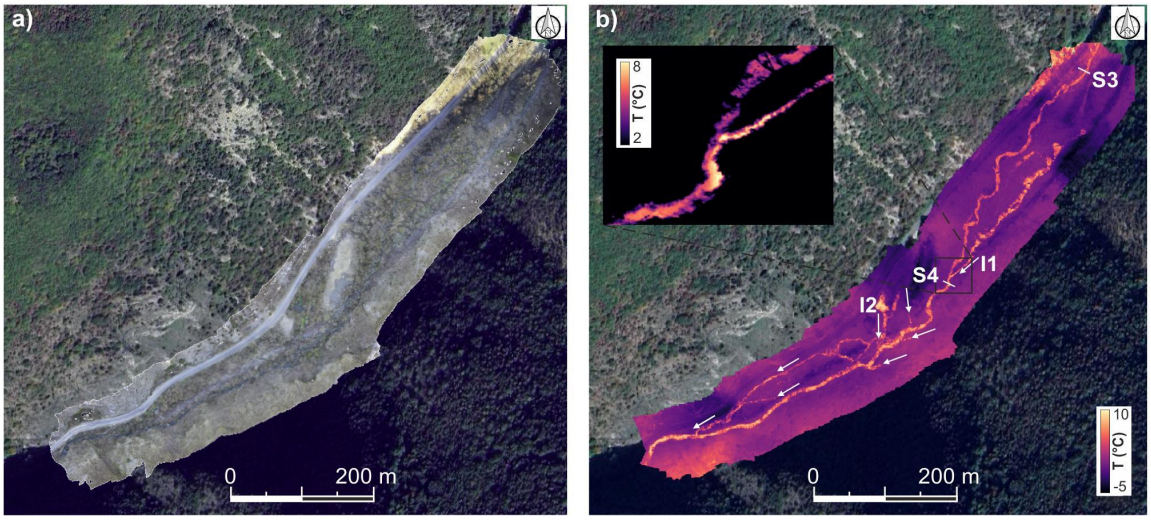

Figure 6: a) optical, and b) thermal drone investigations carried out in January 2024. Base map: map data © 2025 Google.

https://doi.org/10.5194/egusphere-2025-4368
Preprint. Discussion started: 8 October 2025

3.2 Hydrochemical and isotopic characterization of Ussita stream waters

The results of the systematic, approximately monthly campaigns from November 2023 to July 2024 for major soluble ions and other physical parameters (streamflow, temperature, pH, and electrical conductivity) are shown in Table S4. Regarding the isotopic composition of stable water isotopes, Table S5 displays the δD and $\delta^{18}O$ composition of rain and stream waters sampled approximately monthly from June 2023 to March 2024.

The analytical uncertainty of the chemical analyses for major soluble ions was evaluated using the Charge Balance Error (CBE), which checks that the total sum of all positive charges (cations) matches the total sum of all negative charges (anions). For data in Table S4, the average CBE is 2.8%, which remains well within the commonly accepted limit of ±5%. For further details about the average and coefficient of variation of measures of each sampling point, refer to Table S6, for the major soluble ions, and to Table S7, for the stable water isotopes.

Figure 7a shows the Langelier-Ludwig diagram for the Ussita stream water, highlighting a bicarbonate earth-alkaline composition typical of water interacting with carbonates, which is consistent with the lithological composition of the Ussita catchment (see Figure 1). As shown in Figs. 7b,c, moving from site S1 to S5, the stream water's sulfate and magnesium contents increase (Figs. 7b,c), indicating two distinctly different hydrotypes. Specifically, there is a notable increase in sulfate and magnesium levels in the lower part of the stream (S5) compared to the upper sections (S1, S2, S3). Data reveal a more alkaline composition for S1, S2, and S3 stream water, while S5, along with I1 and I2, shows a less alkaline and slightly more sulfate-chloride composition (Fig. 7d).

https://doi.org/10.5194/egusphere-2025-4368
Preprint. Discussion started: 8 October 2025

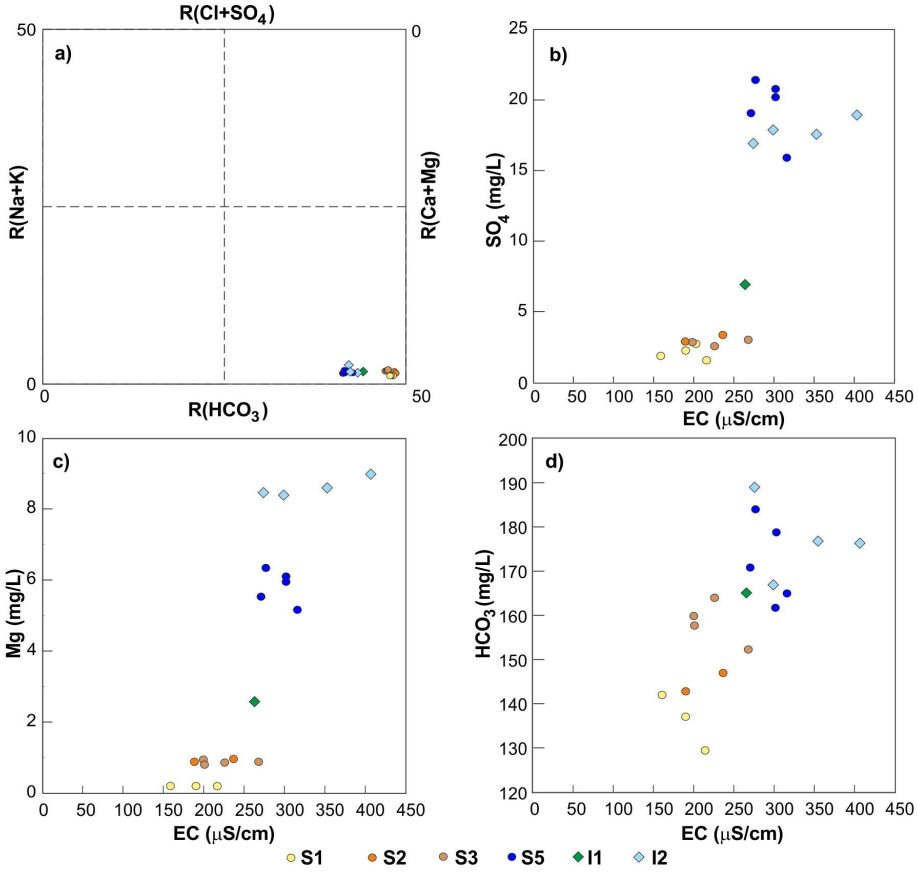

Figure 7: a) Langelier-Ludwig diagram for the Ussita stream; b) sulphate concentrations vs EC values; c) Magnesium concentrations vs EC values; d) Alkalinity vs EC values. For the location of sampling points, see Fig. 1.

Figure 8a displays the isotopic composition of water (i.e., δD and $\delta^{18}O$) at the sampling points, in relation to the Local Meteoric Water Line (LMWL), estimated from the isotopic composition of Ussita precipitation waters (PR1, PR2, PR3, and PR4), the Global Meteoric Water Line (GMWL; Craig, 1961), and the Mediterranean Meteoric Water Line (MMWL; Longinelli and Selmo, 2003).

https://doi.org/10.5194/egusphere-2025-4368
Preprint. Discussion started: 8 October 2025

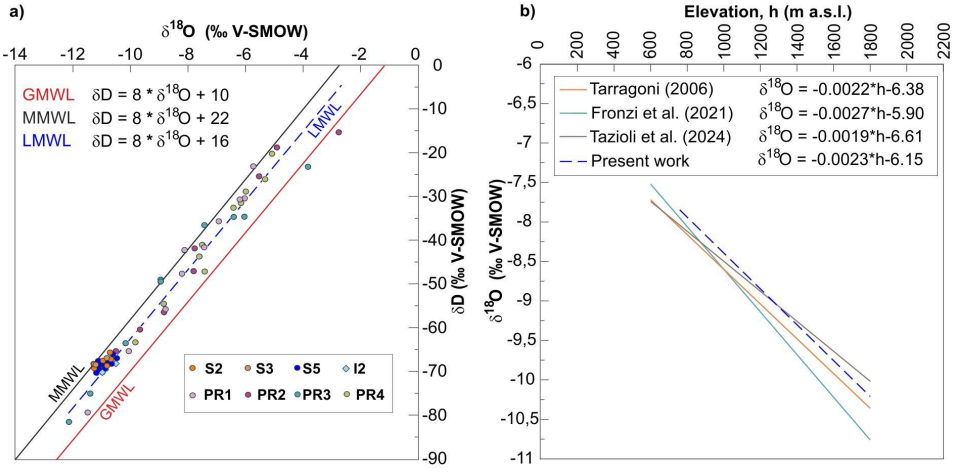

505 **Figure 8: a) δD vs δ^{18}O values of precipitation samples with the resulting linear regression (Local Meteoric Water Line, LMWL), compared with the Global Meteoric Water Line (GMWL) and the Mediterranean Meteoric Water Line (MMWL); b) Linear regression between δ^{18}O and elevation determined by four water collectors (PR) with those proposed by Tarragoni (2006), Fronzi et al. (2021), and Tazioli et al. (2024). For the location of sampling points, see Fig. 1.**

510 Figure 8a, as well as Table S5, show that overall, the precipitation values of δD and δ^{18}O are more negative than those of stream waters. Moreover, precipitation values exhibit the highest variations of cv (from 35% to 47% for δD to 22% to 35% for δ^{18}O) with respect to cv in stream waters (from 1% to 3%).

Stream water samples show lc-excess values ranging from 0.41‰ to 6.04‰, with a standard deviation of 1.40‰ (see Table S4), and average and median lc-excess values are 2.75‰ and 2.74‰, respectively. Table S5 highlights that within each
515 sampling point, the lc-excess average values range from 1.01 ‰ (I2) to 3.42 ‰ (S2) with quite high CV values (from 38% to 84%, Table S6). These generally positive lc-excess values indicate rapid infiltration of rainwater, which prevents isotopic fractionation typically caused by evapotranspiration processes often associated with more negative lc-excess values (Sprenger et al., 2016). This supports the hypothesis of rapid and direct recharge of meteoric water into the groundwater system, as well as a significant contribution of groundwater to the baseflow of the Ussita stream.

520 Because this rapid infiltration minimizes fractionation and preserves the isotopic signature from precipitation (input) to stream discharge (output), once the δ^{18}O - elevation relationship was established (see Fig. 8b, blue dashed line), this relationship was used to compute the Isotope Recharge Elevation (CIRE) values for the S1 and S5 sampling points, yielding elevations of 1855 m a.s.l. for S1 and 2193 m a.s.l. for S5.

These estimates were also compared with values derived from previously published δ^{18}O-elevation relationships in the Mt.
525 Sibillini area, specifically those reported by Tarragoni (2016), Fronzi et al. (2021), and Tazioli et al. (2024) (equations also shown in Fig. 8b). Based on all available relationships, the CIRE values ranged between 1672–1855 m a.s.l. for S1 and 1960–2193 m a.s.l. for S5.

https://doi.org/10.5194/egusphere-2025-4368
Preprint. Discussion started: 8 October 2025

3.3 Integrated approaches for computing the water budget and recharge area

The mean annual water budget was carried out over the MDU catchment (A = 44 km^2) using Eq. 7, referring to the 2019-2023 period. The unknown component ($Q_{in}^{gw} - Q_{out}^{gw}$) and the Q/WS ratio - by the approach of Schaller and Fan (2009) - were calculated.

All water budget components are presented in Mm^3/year. The mean streamflow at S5, i.e., the catchment closure (Q), yields approximately 29.6 Mm^3/year. The mean change in storage (ΔS), calculated by analyzing the stream recession curves for each year and applying Eq. 6 proposed by Korkmaz (1990), resulted in a mean annual volume of about -0.964 Mm^3/year. The following subsections report the results from the two water budget experiments (Case I and Case II), as detailed in section 2.7.3. In both cases, the recharge area is estimated using Eq. 11.

3.3.1 Results of Case I

Table 1 shows the results of the Case I water budget, considering P_{rain}, as the only precipitation input, and therefore WS as the recharge. Within the uncertainties of the various water budget components, all the computations reveal that $Q_{in}^{gw} > Q_{out}^{gw}$, indicating that the potential extension of the hydrogeological catchment, computed by Eq. 11, is larger than the catchment one (A* = 54.31±4.38 km^2, compared to A = 44.06 km^2). The presence of groundwater inflow is also confirmed by the Q/WS ratio, which is higher than one for all the products analyzed, reaching a mean value of about 1.25 (i.e., about 25% of the Ussita stream discharge is fed by GW circulation coming from regions outside the catchment). In the computation of A* values, an effective infiltration (I = 0.90*S) over areas exceeding the catchment is considered (i.e., outside the catchment, about 10% of WS contributes to the runoff towards other systems).

Table 1: Water budget results over the MDU catchment (A of about 44 km^2) for the 2019-2023 period, using different ground-based, satellite, and reanalysis products to compute the water surplus (WS). A* indicates the potential extension of the hydrogeological catchment.

P_{rain} products	ET products	Q (Mm^3/year)	ΔS (Mm^3/year)	WS = P_{rain}-ET (Mm^3/year)	$Q_{in}^{gw} - Q_{out}^{gw}$ (Mm^3/year)	Q/WS (-)	A* (km^2)
MCM	MODIS	29.55	-0.964	23.77	4.82	1.24	53.01
	LSAF			25.50	3.09	1.16	49.41
MERIDA	MODIS			24.78	3.81	1.19	50.84
	LSAF			25.71	2.88	1,15	48.99
ERA5	MODIS			20.72	7.87	1.43	60.82
	LSAF			23.00	5.59	1.28	54.77
IMERG	MODIS			20.99	7.60	1.41	60.02
	LSAF			23.89	4.70	1.24	52.74
USSITA weather station	T–M method (FC = 100 mm)			24.70	3.89	1.20	51.01
	T-M method (FC = 150 mm)			23.47	5.12	1.26	53.67

https://doi.org/10.5194/egusphere-2025-4368
Preprint. Discussion started: 8 October 2025

BIGBANG ground-based spatialized rainfall	T–M method			24.77	3.82	1.19	50.86
			Average value	23.76	**4.84**	**1.25±0.09**	**54.31±4.38**

It should be pointed out that among the P_{rain} products in Table 1, the Ussita weather station and rainfall data used by the BIBGANG model refer to heated rain gauges, even if they are located at a very small altitude compared to the mean altitude of the MDU catchment; thus, they are not fully representative of the snow melt contribution at the catchment scale (i.e., the mean altitude is 1315 a.s.l., with the stream headwater characterized by relief reaching an altitude higher than 2000 m a.s.l.).

3.3.2 Results of Case II: the role of snow melting in aquifer recharge

This case consists of eight evaluations obtained by integrating the WS estimations based on P_{rain} as well as P_{snow} estimates based on SWE of IT SNOW, following the approach in Fig. 3. Figure 9 shows the mean daily IT SNOW SWE time series for the 2010-2024 period, highlighting a considerable contribution of snow, especially for the 2022 period. After integrating the snow melt data (P_{snow}) into the WS values, it was possible to recompute the water budget, the results of which are synthesized in Table 2. Considering the contribution of snow melt, the average hydrogeological catchment resulted in 43.02±2.45 km^2, practically similar to the catchment area. It indicates that GW inflows (Q_{in}^{gw}) are negligible, and this highlights the important role of snow melt in the catchment.

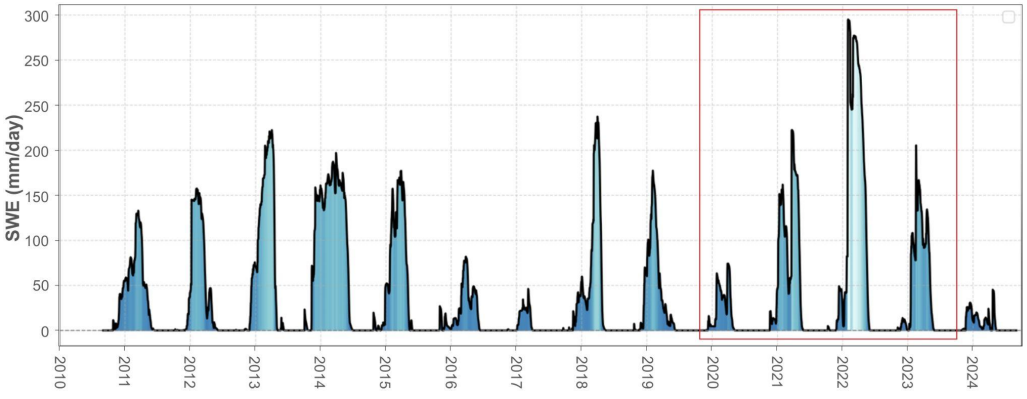

Figure 9: SWE values during the 2010-2024 period for the MDU catchment. The red rectangle represents the period used to compute the water budget.

Table 2: Water budget results over MDU catchments using different ground-based, satellite, and reanalysis products to compute the water surplus (WS), integrated with P_{snow} derived from the IT SNOW dataset. A* indicates the potential extension of the recharge area.

P_{rain} products	**ET products**	**Q (Mm^3/year)**	**ΔS (Mm^3/year)**	**WS + P_{snow} = (P_{rain}-ET)+P_{snow}**	**$Q_{in}^{gw} - Q_{out}^{gw}$ (Mm^3/year)**	**Q/(WS+P_{snow}) (-)**	**A* (km^2)**

https://doi.org/10.5194/egusphere-2025-4368
Preprint. Discussion started: 8 October 2025

				(Mm³/year)			
MCM	MODIS	29.55	-0.964	30.60	-2.01	0.97	41.17
	LSAF			30.89	-2.30	0.96	40.78
MERIDA	MODIS			31.40	-2.81	0.94	40.13
	LSAF			30.66	-2.07	0.96	41.10
ERA5	MODIS			27.81	0.78	1.06	45.31
	LSAF			28.30	0.29	1.04	44.52
IMERG	MODIS			27.18	1.41	1,09	46.35
	LSAF			28.14	0.45	1.05	44.77
			Average value	29.37	**-0.78**	**1.01±0.06**	**43.02±2.45**

4 Discussion

4.1 Integrated approaches to improve understanding of groundwater-surface water interactions

We investigated the processes that control the spatial and temporal dynamics of groundwater–surface water (GW–SW) interactions in a mountainous sector of the Central Apennines by combining ground-based monitoring with remote sensing. As noted by Ma et al. (2024), applying such methods in specific regional contexts is essential for understanding the spatial scales over which they are valid, as well as their respective strengths and limitations. This knowledge is critical for building a reliable and comprehensive picture of the hydrogeological systems that sustain mountain streams. In this study, we employed a suite of complementary techniques—including differential stream gauging, physical hydrograph separation, surface-water tracer tests, and thermal and optical UAV surveys—that align with the best-practice methods identified in the GW/SW Method Selection Tool (GW/SW-MST) developed by Hammett et al. (2022).

In detail, the main advantage of the integrated approach is the investigation of the spatial distribution of GW inflow along the Ussita stream, revealing that most of the baseflow in the stream from S1 to S3 is sustained by the VDP spring (Q ≃ 220 L/s), with a huge baseflow increase between S3 and S5 sections (Q ≃ 650 L/s) delineating, two different sources of alimentation: i) the Maiolica Complex for the VDP spring (EC ≃ 210 µS/cm; SO_4 ≃ 2.5 mg/l), and ii) the Base Limestone Complex for punctual and linear springs downstream of the S3 section and up to S5 (EC ≃ 310 µS/cm; SO_4 ≃ 18.7 mg/l), with some mixing water with intermediate characteristics in the I1 sampling point related to the Maiolica Complex contribution (Ussita left bank, Fig. 1, EC ≃ 264 µS/cm; SO_4 ≃ 6.9 mg/l). Overall, the findings highlights that in the lowest part of the MDU catchment (downstream of S3 up to S5, Fig. 1) the GW circulation feeding the basal linear and punctual springs show clear signs of interactions with low-permeability anhydrites ($CaSO_4$) and dolomites ($CaMg(CO_3)_2$) of the Evaporites Complex underlying the Base Limestone Complex, outcropping in a small tectonic window in the stream's right bank (less than 1 km north to S3 section, see Fig. 5b). This figure confirms that the geological features of the catchment control the hydro-geochemical characteristics of the baseflow (e.g., Farvolden, 1963; Winter, 2001; Bloomfield et al., 2009; Segura et al., 2019). As reported by Levin et al. (2023), measurements made at a point or field scale are not easily extrapolatable to a catchment scale because of the spatial heterogeneity of preferential flow paths.

https://doi.org/10.5194/egusphere-2025-4368
Preprint. Discussion started: 8 October 2025

4.2 Estimation of the recharge area

Although the delineation of the recharge area feeding the basal linear and punctual springs of the Ussita stream remains challenging, the results from the water budget allowed, by using different ground-based, satellite, and re-analysis datasets, to define and constrain its extension (i.e., the area of the hydrogeological basin is close to the catchment one). This finding is confirmed by the isotope data and analysis of CIRE, which indicates recharge elevations of up to 2193 m a.s.l. for the MDU system (at section S5) and 1855 m a.s.l. for the VDP spring (at section S1). These values are consistent with the topographic configuration and the hydrogeological setting of the catchment, confirming that the main recharge occurs in the highest parts of the catchment, above 2000 m a.s.l., where snow accumulation and subsequent melt are most significant. The isotopic composition of stream water ($\delta^{18}O$ and δD), coupled with generally positive lc-excess values (mean = 1.76‰), highlights rapid infiltration with minimal evaporative enrichment, supporting the hypothesis of direct recharge by meteoric waters. The $\delta^{18}O$ further supports the spatial pattern of recharge-elevation regression line, which matches previous studies in the area (Tarragoni, 2006; Fronzi et al., 2021; Tazioli et al., 2024), confirming the robustness of this approach in mountainous carbonate contexts. Additionally, the recharge elevations inferred from CIRE align well with the hydrochemical shift observed between S3 and S5, where a marked increase in sulphate and magnesium concentrations reflects the influence of deeper groundwater flow paths interacting with the Evaporites Complex. The isotopic evidence allows us to constrain both the origin and the altitude of recharge areas, providing an independent validation of the hydrological processes inferred from water budget modeling and hydrochemical results. The delineation of the recharge area for both the MDU and VDP sectors is further corroborated by the results of multiple dye tracer tests conducted in the region by several authors (Nanni et al. 2020; Fronzi et al. 2020; Fronzi et al. 2021; Cambi et al. 2022; Mammoliti et al. 2022). These studies, based on six artificial tracer tests, revealed that the Ussita catchment shows no evidence of groundwater input from areas outside its hydrological boundaries, reinforcing the hypothesis of a predominantly internal recharge regime. The evaluation of the recharge area is a key aspect for mountain regions, considering that using rain gauges alone is particularly problematic because they are systematically installed at lower elevations and are not representative of high-elevation precipitation and heterogeneous snowfall patterns (Cambi et al., 2010; Daly et al., 2017; Ly et al., 2013; Di Matteo et al., 2017).

Overall, the GW contribution in the MDU system (i.e., the average baseflow given as specific discharge, q) was estimated to be about 22 L/s/km^2, a value falling in the range of 18-24 L/s/km^2, as obtained by Boni et al. (1986) for rivers fed by carbonate aquifers in the mountain ridge of Central Italy. Integrating the precipitation range in the area derived from the different estimations (mean value of about 1000 mm/year), the specific discharge of the Ussita catchment falls in the class III (humid areas) based on the global distribution of carbonate rocks and karst water resources (Goldscheider et al., 2020).

4.3 Importance of snow for aquifer recharge

The contribution of snow melt to the water budget in mountainous regions is still not clearly understood and is challenging to evaluate due to the scarcity of ground-based observation networks. As inferred from the MDU catchment, the role of snow

https://doi.org/10.5194/egusphere-2025-4368
Preprint. Discussion started: 8 October 2025

melt in the recharge of aquifers is significant, accounting for about 20%. This value aligns with recent evaluations conducted on other hydrogeological systems of the Central Apennines. Lorenzi et al. (2023), based on satellite images of snow cover from 2019 to 2022 over the Gran Sasso aquifer, found that snow melt contributed to roughly 15% of the total aquifer recharge, highlighting the importance of snow coverage periods in areas characterized by karst features. Recently, Di Giovanni and Rusi (2024) collected six years of ground-based rainfall and snow cover data from 2018 to 2023 for six carbonate aquifers in Central Italy, ranging from Gran Sasso to Monte Marsicano. Their analysis, using data from seven snow cover measuring stations, revealed that snowmelt contributed between 10% and 30% to total infiltration. Overall, our study emphasizes the good performance of the IT-SNOW datasets in evaluating snowmelt contributions to aquifer recharge in Italian mountain regions. This finding is particularly important given that, over the past decade, snow cover thickness— including in the highest parts of the MDU catchment— has been very low in some years (2016, 2017, 2020, and 2024, Fig. 9). In this context, the observed percentages of aquifer recharge from snowmelt for the MDU catchment and other hydrogeological systems in Central Italy and elsewhere can help address the ongoing question regarding the connection between snowmelt and groundwater flow in snow-dominated regions of the Mediterranean area (e.g., Fayad et al., 2017).

5 Conclusions

This study, conducted in the Ussita catchment, demonstrated how an integrated approach is essential for understanding the complex dynamics of groundwater (GW)-surface water (SW) interactions in fractured carbonate mountain regions. Combining different methods provided a comprehensive understanding of the hydrogeological system. Hydrochemical and isotopic analyses helped distinguish between various water sources, while thermal drone surveys and stream discharge measurements accurately mapped zones of groundwater inflow into the stream that were otherwise hidden by dense riverine vegetation. Stream stretches fed by aquifer hosted in the Maiolica Complex (MAC) were carefully evaluated compared to those in the Basal Limestone Complex (BLC). In detail, aquifers in the MAC feed the VDP spring in the catchment headwaters, which mainly sustain the stream discharge at the Ussita Village catchment (Base Flow Index, BFI = 80%). On the contrary, moving downstream to the catchment outlet (Madonna dell'Uccelletto catchment, MDU), the role of BLC in feeding the stream prevails, and the BFI increases to 90%. This is a crucial finding in systems characterized by diverse lithologies and complex tectonic structures, where the preferential flow paths of groundwater are often difficult to map. This detailed mapping of GW-SW water interactions is vital for understanding the hydrological connectivity of gaining streams. Proper interpretation of in-situ monitoring data alongside satellite-based products enables the combination of multiple datasets to better constrain the water budget and recharge areas by accounting for both rain and snowmelt inputs. Specifically, the water budget computed from these datasets showed that snowmelt contributed approximately 20% to aquifer recharge during the 2019-2024 period, emphasizing that if the release of water from a traditional snowpack decreases in the coming years, it would affect GW availability and, consequently, stream discharge, posing a multifaceted challenge for maintaining ecosystems and human water supplies. In conclusion, the techniques and methods used for the Ussita stream can serve as a model for guiding field campaigns

https://doi.org/10.5194/egusphere-2025-4368
Preprint. Discussion started: 8 October 2025

in other catchments, aiming to identify site-specific conditions responsible for GW inflow, from the point source to the stream stretch.

Data availability

Most of the data used in the paper are in the Supplementary Materials. The corresponding authors can provide all raw data upon request.

Author contribution

LDM, DV, MD, IM, and CM designed the conceptualization and methodology; All the authors contributed to data curation; SO, LDM, DV, MD, DF, JG, IM, PF, and CM carried out the formal analysis and visualization; LDM, IM, JG, and CM provided the financial support; All the authors contributed to writing the original draft and revising and editing it; LDM and CM supervised the research activities.

Competing interests

The authors declare that they have no conflict of interest.

Acknowledgements

We thank Dr. Francesco Capecchiacci for water isotopic analyses (Laboratorio di Geochimica degli Isotopi Stabili, Dipartimento di Scienze della Terra, Università degli Studi di Firenze) and Prof. David Michele Cappelletti for water physical-chemical analyses (Laboratorio TRACES - Trace Analysis for Chemical Speciation, Dipartimento di Chimica, Biologia e Biotecnologie, Università degli Studi di Perugia).

Financial support

This work was supported by the research projects: Resilience and vulnerability of water resources under drought conditions – new insights from integrated in-situ and remote sensing approaches revolution (REVULUTION, 2023–2025), Joint Bilateral Agreement CNR/Royal Society of London (UK) Biennial Programme 2023–2025 (IEC\R2\232027); Hydrological Controls on Carbonate-mediated CO2 Consumption – Hydro4C (code 2022PFNNRS_PE10_PRIN2022, Protocol 2022PFNNRS), funded by the European Union – Next Generation EU (CUP J53D23002840006, Protocollo 2022PFNNRS); Analisi dei processi idrogeologici ed idromorfologici nel contesto dei cambiamenti climatici ed antropici (grant number RICATENEO2024DIMATTEO).

https://doi.org/10.5194/egusphere-2025-4368
Preprint. Discussion started: 8 October 2025

References

Miller, B. B. and Carter, C.: The test article, J. Sci. Res., 12, 135–147, doi:10.1234/56789, 2015.

Smith, A. A., Carter, C., and Miller, B. B.: More test articles, J. Adv. Res., 35, 13–28, doi:10.2345/67890, 2014.

Acreman, M. C., and Dunbar, M. J.: Defining environmental river flow requirements–a review, HESS, 8(5), 861-876, doi:10.5194/hess-8-861-2004, 2004.

Adler, C. , Wester, P., Bhatt, I., Huggel, C., Insarov, G., Morecroft, M., Muccione, V., Prakash, A., Alcántara-Ayala, I., Allen, S. K., Bader, M., Bigler, S., Camac, J., Chakraborty, R., Sanchez, A. C., Cuvi, N., Drenkhan, F., Hussain, A., Maharjan, A., Marchant, R., McDowell, G., Morin, S., Niggli, L., Ochoa, A., Pandey, A., Postigo, J., Razanatsoa, E., Rudloff, V. M., Scott, C., Stevens, M., Stone, D., Thorn, J. P. R., Thornton, J., Viviroli, D. and Werners, S.: Cross-chapter paper 5: mountains, in H.-O., Pörtner, D. C., Roberts, M. M. B., Tignor, E., Poloczanska, K., Mintenbeck, A., Alegría, M., Craig, S., Langsdorf, S., Löschke, V., Möller, A., Okem and B., Rama (eds), Climate change 2022: impacts, adaptation, and vulnerability : Contribution of Working Group II to the Sixth Assessment Report of the Intergovernmental Panel on Climate Change, Cambridge University Press, Cambridge, 2273-2318, doi:10.1017/9781009325844.022, 2023.

Allen, R. G., Pereira, L. S., Raes, D. and Smith, M.: FAO Irrigation and drainage paper No. 56, Rome: food and agriculture organization of the United Nations, 56(97), e156, ISBN 92-5-104219-5, 1998.

Alvarez, W.: A review of the Earth history record in the Cretaceous, Paleogene, and Neogene pelagic carbonates of the Umbria-Marche Apennines (Italy): Twenty-five years of the Geological Observatory of Coldigioco. In C., Koeberl and D. M., Bice (Eds.), 250 Million Years of Earth History in Central Italy: Celebrating 25 Years of the Geological Observatory of Coldigioco, GSA, 542, doi:10.1130/2019.2542(01), 2019.

Avanzi, F., Gabellani, S., Delogu, F., Silvestro, F., Pignone, F., Bruno, G., Pulvirenti, L., Squicciarino, G., Fiori, E., Rossi, L., Puca, S., Toniazzo, A., Giordano, P., Falzacappa, M., Ratto, S., Stevenin, H., Cardillo, A., Fioletti, M., Cazzuli, O., Cremonese, E., Morra di Cella, U. and Ferraris, L.: IT-SNOW: a snow reanalysis for Italy blending modeling, in situ data, and satellite observations (2010–2021), Earth Syst. Sci. Data, 15, 639-660, doi:10.5194/essd-15-639-2023, 2023.

Avanzi, F., Munerol, F., Milelli, M., Gabellani, S., Massari, C., Girotto, M., Cremonese, E., Galvagno, M., Bruno, G., Mora di Cella, U., Rossi, L., Altamura, M. and Ferraris, L.: Winter snow deficit was a harbinger of summer 2022 socio-hydrologic drought in the Po Basin, Italy, Commun. Earth Environ., 5(1), 64, doi:10.1038/s43247-024-01222-z, 2024.

Azimi, S., Massari, C., Formetta, G., Barbetta, S., Tazioli, A., Fronzi, D., Modanesi, S., Tarpanelli, A. and Rigon, R.: On understanding mountainous carbonate basins of the Mediterranean using parsimonious modeling solutions, HESS, 27(24), 4485-4503, doi:10.5194/hess-27-4485-2023, 2023.

Bloomfield, J. P., Allen, D. J. and Griffiths, K. J.: Examining geological controls on baseflow index (BFI) using regression analysis: An illustration from the Thames Basin, UK. J. Hydrol., 373(1-2), 164-176, doi:10.1016/j.jhydrol.2009.04.025, 2009.

https://doi.org/10.5194/egusphere-2025-4368
Preprint. Discussion started: 8 October 2025

Bonacci, O.: Karst springs hydrographs as indicators of karst aquifers, Hydrol. Sci. J., 38(1), 51-62, doi:10.1080/02626669309492639,1993.

Bonanno, R., Lacavalla, M. and Sperati, S.: A new high-resolution meteorological reanalysis Italian dataset: MERIDA, Q. J. R. Meteorol. Soc., 145(721), 1756-1779, doi:10.1002/qj.3530, 2019.

Boni, C. F., Bono, P., and Capelli, G.: Carta idrogeologica (scala 1: 500,000); B) Carta idrologica (scala 1: 500,000); C) Carta dei bilanci idrogeologici e delle risorse idriche sotterranee (scala 1: 1,000,000), Mem. Soc. Geol. It., 35, 991-1012, 1986.

Boni, C., Baldoni, T., Banzato, F., Cascone, D., and Petitta, M.: Hydrogeological study for identification, characterisation and management of groundwater resources in the Sibillini Mountains National Park (Central Italy), IJEGE, 2, 21-39, doi:10.4408/IJEGE.2010-02.O-02, 2010.

Braca, G., Mariani, S., Lastoria, B., Tropeano, R., Casaioli, M., Piva, F., Marchetti, G. and Bussettini, M.: Bilancio idrologico nazionale: stime BIGBANG e indicatori sulla risorsa idrica, Update 2023, Report n. 401/2024, ISPRA, Roma, ISBN: 978-88-448-1232-4, 2024.

Brozzetti, F., Boncio, P., Cirillo, D., Ferrarini, F., De Nardis, R., Testa, A., Liberi, F., and Lavecchia, G.: High-resolution field mapping and analysis of the August–October 2016 coseismic surface faulting (central Italy earthquakes): Slip distribution, parameterization, and comparison with global earthquakes, Tectonics, 38(2), 417-439, doi:10.1029/2018TC005305, 2019.

C3S: Copernicus Climate Change Service: ERA5-Land monthly averaged data from 1950 to present. Copernicus Climate Change Service (C3S) Climate Data Store (CDS), doi:10.24381/cds.68d2bb30, 2022, (Accessed on 28-04-2025).

Cambi, C., Valigi, D. and Di Matteo, L.: Hydrogeological study of data-scarce limestone massifs: the case of Gualdo Tadino and Monte Cucco structures (central Apennines, Italy), Boll. Geofis. Teor. Appl., 51(4), 2010.

Cambi, C., Mirabella, F., Petitta, M., Banzato, F., Beddini, G., Cardellini, C., Fronzi, D., Mastrolillo, L., Tazioli, A. and Valigi, D.: Reaction of the carbonate Sibillini Mountains Basal aquifer (Central Italy) to the extensional 2016–2017 seismic sequence, Sci. Rep., 12(1), 22428, doi:10.1038/s41598-022-26681-2, 2022.

Carlotto, T. and Chaffe, P. L. B.: Master recession curve parameterization tool (MRCPtool): different approaches to recession curve analysis, Comput. Geosci, 132, 1-8, doi:10.1016/j.cageo.2019.06.016, 2019.

Carrillo-Rivera, J.: Application of the groundwater-balance equation to indicate interbasin and vertical flow in two semi-arid drainage basins, Mexico, Hydrogeol. J., 8(5), 503-520, doi:10.1007/s100400000093, 2000.

Chapman, T. G.: Comment on "Evaluation of automated techniques for base flow and recession analyses" by R.J., Nathan and T.A., McMahon, Water Resour. Res., 27(7), 1783-1784, doi:10.1029/91WR01007,1991.

Chiodini, G., Caliro, S., Avino, R., Bini, G., Giudicepietro, F., De Cesare, W., Ricciolino, P., Aiuppa, A., Cardellini, C., Petrillo, Z., Selva, J., Siniscalchi, A. and Tripaldi, S.: Hydrothermal pressure-temperature control on CO2 emissions and seismicity at Campi Flegrei (Italy), J. Volcanol. Geotherm. Res., 414, 107245, doi:10.1016/j.jvolgeores.2021.107245, 2021.

Conant Jr, B., Robinson, C. E., Hinton, M. J., and Russell, H. A.: A framework for conceptualizing groundwater-surface water interactions and identifying potential impacts on water quality, water quantity, and ecosystems, J. Hydrol., 574, 609-627, doi:10.1016/j.jhydrol.2019.04.050, 2019.

https://doi.org/10.5194/egusphere-2025-4368
Preprint. Discussion started: 8 October 2025

Costantini, E. A. C., G. L'Abate, R. Barbetti, M. Fantappié, R. Lorenzetti, S. Magini: Soil Map of Italy, Consiglio per ricerca e la sperimentazione in agricoltura, Ministero delle Politiche Agricole Alimentari e Forestali, https://esdac.jrc.ec.europa.eu/images/Eudasm/IT/2012Carta_Suoli_Italia.jpg, 2012 (Accessed on 06-05-2025).

Craig, H.: Isotopic variations in meteoric waters. Science, 133(3465), 1702-1703, doi:10.1126/science.133.3465.1702, 1961.

Daly, C., Slater, M. E., Roberti, J. A., Laseter, S. H. and Swift Jr, L. W.: High-resolution precipitation mapping in a mountainous watershed: ground truth for evaluating uncertainty in a national precipitation dataset, Int. J. Climatol., 37, 124-137, doi:10.1002/joc.4986, 2017.

Dettinger, M.: Impacts in the third dimension, Nat. Geosci., 7(3), 166-167, doi:10.1038/ngeo2096, 2014.

Di Domenicantonio, A., Cassiani, B., Ruisi, M. and Traversa, P.: Quantitative hydrogeology in the Tevere River basin management planning (central Italy), IJEGE, 1, 69-82, doi:10.4408/IJEGE.2009-01.O-04, 2009.

Di Matteo, L., Dragoni, W., Maccari, D. and Piacentini, S. M.: Climate change, water supply and environmental problems of headwaters: The paradigmatic case of the Tiber, Savio and Marecchia rivers (Central Italy), STOTEN, 598, 733-748, doi:10.1016/j.scitotenv.2017.04.153, 2017.

Di Matteo, L., Dragoni, W., Azzaro, S., Pauselli, C., Porreca, M., Bellina, G. and Cardaci, W.: Effects of earthquakes on the discharge of groundwater systems: The case of the 2016 seismic sequence in the Central Apennines, Italy, J. Hydrol., 583, 124509, doi:10.1016/j.jhydrol.2019.124509, 2020.

Di Matteo, L., Capoccioni, A., Porreca, M. and Pauselli, C.: Groundwater-surface water interaction in the Nera River Basin (Central Italy): new insights after the 2016 seismic sequence, Hydrology, 8(3), 97, doi:10.3390/hydrology8030097, 2021.

Donnini, M., Frondini, F., Probst, J. L., Probst, A., Cardellini, C., Marchesini, I. and Guzzetti, F.: Chemical weathering and consumption of atmospheric carbon dioxide in the Alpine region, Glob. planet. change, 136, 65-81, doi:10.1016/j.gloplacha.2015.10.017, 2016.

Donnini, M., Benigni, A., Dionigi, M., Massari, C., Cappelletti, D., Selvaggi, R., Fastelli, M., Scricciolo, E., Cencetti, C. and Marchesini, I.: Hydrology and atmospheric CO2 consumption by chemical weathering in a Mediterranean watershed, Catena, 252, 108868, doi:10.1016/j.catena.2025.108868, 2025.

Dragoni, W., Mottola, A. and Cambi, C.: Modeling the effects of pumping wells in spring management: the case of Scirca spring (central Apennines, Italy), J. Hydrol., 493, 115-123, doi:10.1016/j.jhydrol.2013.03.032, 2013.

Duncan, H. P.: Baseflow separation–A practical approach, J. Hydrol., 575, 308-313, doi:10.1016/j.jhydrol.2019.05.040, 2019.

Farvolden, R. N.: Geologic controls on ground-water storage and base flow, J. Hydrol., 1(3), 219-249, doi:10.1016/0022-1694(63)90004-0, 1963.

Fayad, A., Gascoin, S., Faour, G., López-Moreno, J. I., Drapeau, L., Le Page, M. and Escadafal, R.: Snow hydrology in Mediterranean mountain regions: A review, J. Hydrol., 551, 374-396, doi:10.1016/j.jhydrol.2017.05.063, 2017.

Fernández-Martínez, M., Barquin, J., Bonada, N., Cantonati, M., Churro, C., Corbera, J., Delgado, C., Dulsat-Masvidal, M., Garcia, G., Margalef, O., Pascual, R., Peñuelas J., Preece, C., Sabater, F., Seiler, H., Zamora-Marín, J. M. and Romero,

https://doi.org/10.5194/egusphere-2025-4368
Preprint. Discussion started: 8 October 2025

E.: Mediterranean springs: Keystone ecosystems and biodiversity refugia threatened by global change, GCB, 30(1), e16997, doi:10.1111/gcb.16997, 2024.

Filippini, M., Stumpp, C., Nijenhuis, I., Richnow, H. H. and Gargini, A.: Evaluation of aquifer recharge and vulnerability in an alluvial lowland using environmental tracers, J. Hydrol., 529, 1657-1668, doi:10.1016/j.jhydrol.2015.07.055, 2015.

Frondini, F., Cardellini, C., Caliro, S., Beddini, G., Rosiello, A. and Chiodini, G.: Measuring and interpreting CO2 fluxes at regional scale: the case of the Apennines, Italy, J. Geol. Soc., 176(2), 408-416, doi:10.1144/jgs2017-169, 2019.

Fronzi, D., Di Curzio, D., Rusi, S., Valigi, D. and Tazioli, A.: Comparison between periodic tracer tests and time-series analysis to assess mid-and long-term recharge model changes due to multiple strong seismic events in carbonate aquifers, Water, 12(11), 3073, doi:10.3390/w12113073, 2020.

Fronzi, D., Mirabella, F., Cardellini, C., Caliro, S., Palpacelli, S., Cambi, C., Caliro, S., Palpacelli, S., Cambi, C., Valigi, D. and Tazioli, A.: The role of faults in groundwater circulation before and after seismic events: Insights from tracers, water isotopes and geochemistry, Water, 13(11), 1499, doi:10.3390/w13111499, 2021.

Furey, P. R. and Gupta, V. K.: A physically based filter for separating base flow from streamflow time series, Water Resour. Res., 37(11), 2709-2722, doi:10.1029/2001WR000243, 2001.

Gallego, F., Sans, G. C., Di Bella, C. M., Tiscornia, G. and Paruelo, J. M.: Performance of real evapotranspiration products and water yield estimations in Uruguay, RSASE, 32, 101043, doi:10.1016/j.rsase.2023.101043, 2023.

Gao, H., Tang, Q., Ferguson, C.R., Wood, E.F. and Lettenmaier, D.P.: Estimating the water budget of major US river basins via remote sensing International, J. Remote Sens, 31, 3955–3978, doi:10.1080/01431161.2010.483488, 2010.

Gentilucci, M., Bufalini, M., D'Aprile, F., Materazzi, M. and Pambianchi, G.: Comparison of data from rain gauges and the IMERG product to analyse precipitation in mountain areas of central Italy, IJGI, 10(12), 795, doi:10.3390/ijgi10120795, 2021.

Girotto, M., Formetta, G., Azimi, S., Bachand, C., Cowherd, M., De Lannoy, G., Lievens, H., Modanesi, S., Raleigh, M. S., Rigon, R. and Massari, C.: Identifying snowfall elevation patterns by assimilating satellite-based snow depth retrievals, STOTEN, 906, 167312, doi:10.1016/j.scitotenv.2023.167312, 2024.

Goldscheider, N., Chen, Z., Auler, A. S., Bakalowicz, M., Broda, S., Drew, D., Hartmann, J., Jiang, G., Moosdorf, N., Stevanovic, Z. and Veni, G.: Global distribution of carbonate rocks and karst water resources, Hydrogeol. J., 28(5), 1661-1677, doi:10.1007/s10040-020-02139-5, 2020.

Gregor, M. and Malik, P.: Construction of master recession curve using genetic algorithms, J. Hydrol. Hydromech., 60(1), 3, doi:10.2478/v10098-012-0001-8, 2012.

Hammett, S., Day-Lewis, F. D., Trottier, B., Barlow, P. M., Briggs, M. A., Delin, G., Harvey, J. W, Johnson, C. D., Lane jr., J. W., Rosenberry, D. O. and Werkema, D. D.: GW/SW-MST: A groundwater/surface-water method selection tool, Groundwater, 60(6), 784-791, doi:10.1111/gwat.13194, 2022.

https://doi.org/10.5194/egusphere-2025-4368
Preprint. Discussion started: 8 October 2025

Hartmann, J., Jansen, N., Dürr, H. H., Kempe, S. and Köhler, P.: Global CO2-consumption by chemical weathering: What is the contribution of highly active weathering regions?, Glob. planet. change, 69(4), 185-194, doi:10.1016/j.gloplacha.2009.07.007, 2009.

Healy, R.W., Winter, T.C., LaBaugh, J.W. and Franke, O.L.: Water budgets: Foundations for effective water resources and environmental management: U.S. Geological Survey Circular 1308, 90 p. https://water.usgs.gov/watercensus/AdHocComm/Background/WaterBudgets-FoundationsforEffectiveWater-ResourcesandEnvironmentalManagement.pdf, 2007. (Accessed on 13-05-2025)

Hilton, R. G. and West, A. J.: Mountains, erosion and the carbon cycle, Nat Rev Earth Environ., 1(6), 284-299, doi:10.1038/s43017-020-0058-6, 2020.

Huffman G.J., Stocker E.F., Bolvin D.T., Nelkin E.J. and Tan J.: GPM IMERG Final Precipitation L3 1 day 0.1 degree x 0.1 degree V07, Edited by Andrey Savtchenko, Greenbelt, MD, Goddard Earth Sciences Data and Information Services Center (GES DISC), doi:10.5067/GPM/IMERGDF/DAY/07, 2023. (Accessed on 24-05-2025).

Kang, T., Lee, S., Lee, N. and Jin, Y.: Baseflow separation using the digital filter method: Review and sensitivity analysis, Water, 14(3), 485, doi:10.3390/w14030485, 2022.

Kirchner, J. W.: Catchments as simple dynamical systems: Catchment characterization, rainfall-runoff modeling, and doing hydrology backward, Water Resour. Res., 45(2), doi:10.1029/2008WR006912, 2009.

Korkmaz, N.: The estimation of groundwater recharge from spring hydrographs, Hydrol. Sci. J., 35(2), 209-217, doi:10.1080/02626669009492419, 1990.

Kump, L. R., Brantley, S. L. and Arthur, M. A.: Chemical weathering, atmospheric CO2, and climate, Ann Rev Earth Planet Sci., 28(1), 611-667, doi:10.1146/annurev.earth.28.1.611, 2000.

Lancia, M., Petitta, M., Zheng, C. and Saroli, M.: Hydrogeological insights and modelling for sustainable use of a stressed carbonate aquifer in the Mediterranean area: From passive withdrawals to active management, J. Hydrol. Reg. Stud., 32, 100749, doi:10.1016/j.ejrh.2020.100749, 2020.

Ladson, A. R., Brown, R., Neal, B. and Nathan, R.: A standard approach to baseflow separation using the Lyne and Hollick filter, Australas. J. Wat. Reso., 17(1), 25-34, doi:10.7158/13241583.2013.11465417, 2013.

Landwehr J. M. and Coplen T. B.: Line-conditioned excess: a new method for characterizing stable hydrogen and oxygen isotope ratios in hydrologic systems. In Isotopes in Environmental Studies, Aquatic Forum 2004, IAEA–CSP–26, International Atomic Energy Agency: Vienna, 132-135, ISBN 92–0–111305–X, 2006.

Levin, S. B., Briggs, M. A., Foks, S. S., Goodling, P. J., Raffensperger, J. P., Rosenberry, D. O., Scholl, M. A., Tiedeman, C. R. and Webb, R. M.: Uncertainties in measuring and estimating water-budget components: Current state of the science, WIREs Water, 10(4), e1646, doi:10.1002/wat2.1646, 2023.

Loglisci, N., Boni, G., Cauteruccio, A., Faccini, F., Milelli, M., Paliaga, G. and Parodi, A.: The role of citizen science in assessing the spatiotemporal pattern of rainfall events in urban areas: a case study in the city of Genoa, Italy, NHESS, 24(7), 2495-2510, doi:10.5194/nhess-24-2495-2024, 2024.

https://doi.org/10.5194/egusphere-2025-4368
Preprint. Discussion started: 8 October 2025

Longinelli, A. and Selmo, E.: Isotopic composition of precipitation in Italy: a first overall map, J. Hydrol., 270(1-2), 75-88, doi:10.1016/S0022-1694(02)00281-0, 2003.

Longobardi, A. and Villani, P: Baseflow index characterization in typical temperate to dry climates: conceptual analysis and simulation experiment to assess the relative role of climate forcing features and catchment geological settings, Hydrol. Res., 54(2), 136-148, doi:10.2166/nh.2023.026, 2023.

Lorenzi, V., Barberio, M. D., Sbarbati, C. and Petitta, M.: Groundwater recharge distribution due to snow cover in shortage conditions (2019–22) on the Gran Sasso carbonate aquifer (Central Italy), Environ. Earth Sci., 82(9), 206, doi:10.1007/s12665-023-10889-0, 2023.

Lorenzoni, M., Carosi, A., Giovannotti, M., La Porta, G., Splendiani, A. and Barucchi, V. C.: Ecology and conservation of the Mediterranean trout in the central Apennines (Italy), J. Limnol., 78(1), doi:10.4081/jlimnol.2018.1806, 2019.

Lv, M., Ma, Z., Yuan, X., Lv, M., Li, M. and Zheng, Z.: Water budget closure based on GRACE measurements and reconstructed evapotranspiration using GLDAS and water use data for two large densely-populated mid-latitude basins, J. Hydrol., 547, 585-599, http://dx.doi.org/10.1016/j.jhydrol.2017.02.027, 2017.

Ly, S., Charles, C. and Degré, A.: Different methods for spatial interpolation of rainfall data for operational hydrology and hydrological modeling at watershed scale: a review, BASE, 17(2), https://hdl.handle.net/2268/136084, 2013.

Lyne, V. and Hollick, M.: Stochastic time-variable rainfall-runoff modelling. In Institute of engineers Australia national conference, 79(10), 89-93, Barton, Australia: Institute of Engineers Australia, 1979.

Ma, R., Chen, K., Andrews, C. B., Loheide, S. P., Sawyer, A. H., Jiang, X., Briggs, M. A., Cook, P. G., Gorelick, S. M., Prommer, H., Scanlon, B. R., Guo, Z. and Zheng, C.: Methods for quantifying interactions between groundwater and surface water, Annu. Rev. Environ. Resour., 49, doi:10.1146/annurev-environ-111522-104534, 2024.

Maillet, E.: Essai d'hydraulique souterraine et fluviale: Librairie scientifique, Paris: A. Hermann, 1905.

Mammoliti, E., Fronzi, D., Mancini, A., Valigi, D. and Tazioli, A.: WaterbalANce, a WebApp for Thornthwaite–Mather Water Balance Computation: comparison of applications in two European watersheds, Hydrology, 8(1), 34, doi:10.3390/hydrology8010034, 2021.

Mammoliti, E., Fronzi, D., Cambi, C., Mirabella, F., Cardellini, C., Patacchiola, E., Tazioli, A., Caliro, S. and Valigi, D.: A holistic approach to study groundwater-surface water modifications induced by strong earthquakes: The case of Campiano catchment (Central Italy), Hydrology, 9(6), 97, doi:10.3390/hydrology9060097, 2022.

Marti, E., Leray, S., Villela, D., Maringue, J., Yáñez, G., Salazar, E., Poblete, F., Jimenez, J., Reyes, G., Poblete, G., Huamán, Z., Figueroa, R., Vargas, J. A., Sanhueza, J., Muñoz, M., Charrier, R. and Fernández, G.: Unravelling geological controls on groundwater flow and surface water-groundwater interaction in mountain systems: A multi-disciplinary approach J. Hydrol., 623, 129786, doi:10.1016/j.jhydrol.2023.129786, 2023.

Mastrorillo, L., Baldoni, T., Banzato, F., Boscherini, A., Cascone, D., Checcucci, R., Petitta, M. and Boni, C.: Quantitative hydrogeological analysis of the carbonate domain of the Umbria Region (Central Italy), IJEGE, 1, 137-156, doi:10.4408/IJEGE.2009-01.O-08, 2009.

https://doi.org/10.5194/egusphere-2025-4368
Preprint. Discussion started: 8 October 2025

Mastrorillo, L., Saroli, M., Viaroli, S., Banzato, F., Valigi, D. and Petitta, M.: Sustained post-seismic effects on groundwater flow in fractured carbonate aquifers in Central Italy, Hydrol. Process., 34(5), 1167-1181, doi:10.1002/hyp.13662, 2020.

Mastrorillo, L., Viaroli, S. and Petitta, M.: Co-Occurrence of Earthquake and Climatic Events on Groundwater Budget Alteration in a Fractured Carbonate Aquifer (Sibillini Mts.-Central Italy), Water, 15(13), 2355, doi:10.3390/w15132355, 2023.

Mitsch, W. J. and Gosselink, J. G.: The value of wetlands: importance of scale and landscape setting, Ecol. Econ., 35(1), 25-33, doi:10.1016/S0921-8009(00)00165-8, 2000.

Mu, Q., Zhao, M. and Running, S. W.: Improvements to a MODIS global terrestrial evapotranspiration algorithm, Remote Sens. Environ., 115(8), 1781-1800, doi:10.1016/j.rse.2011.02.019, 2011.

Muñoz, R., Vaghefi, S. A., Drenkhan, F., Santos, M. J., Viviroli, D., Muccione, V. and Huggel, C.: Assessing water management strategies in data-scarce mountain regions under uncertain climate and socio-economic changes, IWRM, 38(11), 4083-4100, doi:10.1007/s11269-024-03853-5, 2024.

Muñoz-Sabater, J., Dutra, E., Agustí-Panareda, A., Albergel, C., Arduini, G., Balsamo, G., Boussetta, S., Choulga, M., Harrigan, S., Hersbach, H., Martens, B., Miralles, D. G., Piles, M., Rodríguez-Fernández, N. J., Zsoter, E., Buontempo, C. and Thépaut, J. N.: ERA5-Land: A state-of-the-art global reanalysis dataset for land applications, ESSD, 13(9), 4349-4383, doi:10.5194/essd-13-4349-2021, 2021.

Nagy, E. D., Szilagyi, J. and Torma, P.: Calibrating the Lyne-Hollick filter for baseflow separation based on catchment response time, J. Hydrol., 638, 131483, doi:10.1016/j.jhydrol.2024.131483, 2024.

Nanni, T., Vivalda, P. M., Palpacelli, S., Marcellini, M. and Tazioli, A.: Groundwater circulation and earthquake-related changes in hydrogeological karst environments: A case study of the Sibillini Mountains (central Italy) involving artificial tracers, Hydrogeol. J., 28(7), 2409-2428, doi:10.1007/s10040-020-02207-w, 2020.

Nathan, R. J. and McMahon, T. A.: Evaluation of automated techniques for base flow and recession analyses, Water Resour. Res., 26(7), 1465-1473, doi:10.1029/WR026i007p01465, 1990.

Noor, K., Marttila, H., Klöve, B., Welker, J. M. and Ala-aho, P.: The spatiotemporal variability of snowpack and snowmelt water 18O and 2H isotopes in a subarctic catchment, Water Resour. Res., 59(1), e2022WR033101, doi:10.1029/2022WR033101, 2023.

Ofterdinger, U., MacDonald, A. M., Comte, J. C. and Young, M. E. (eds): Groundwater in fractured bedrock environments: managing catchment and subsurface resources - an introduction, Geological Society, London, Special Publications, 479, 1–9. doi:10.1144/SP479-2018-170, 2019.

Petitta, M., Scarascia Mugnozza, G., Barbieri, M., Bianchi Fasani, G., and Esposito, C.: Hydrodynamic and isotopic investigations for evaluating the mechanisms and amount of groundwater seepage through a rockslide dam, Hydrol. Process., 24(24), 3510-3520, doi:10.1002/hyp.7773, 2010.

Petitta, M., Mastrorillo, L., Preziosi, E., Banzato, F., Barberio, M. D., Billi, A., Cambi, C., De Luca, G., Di Carlo, G., Di Curzio, D., Di Salvo, C., Nanni, T., Palpacelli, S., Rusi, S., Saroli, M., Tallini, M., Tazioli, A., Valigi, D., Vivalda, P. and

https://doi.org/10.5194/egusphere-2025-4368
Preprint. Discussion started: 8 October 2025

Doglioni, C.: Water-table and discharge changes associated with the 2016–2017 seismic sequence in central Italy: hydrogeological data and a conceptual model for fractured carbonate aquifers, Hydrogeol. J., 26(4), 1009-1026, doi:10.1007/s10040-017-1717-7, 2018.

Pierantoni, P., Deiana, G. and Galdenzi, S.: Stratigraphic and structural features of the Sibillini mountains (Umbria-Marche Apennines, Italy), Ital. J. Geosci., 132(3), 497-520, doi:10.3301/IJG.2013.08, 2013.

Pignone, F., Rebora, N., Silvestro, F. and Castelli, F.: GRISO – Rain, CIMA Research Foundation, Savona, Italy, Operational Agreement 778/2009 DPC-CIMA, Year-1 Activity Report 272/2010, 353 pp., 2010.

Pignone, F., Rebora, N. and Silvestro, F.: Modified Conditional Merging technique: a new method to estimate a rainfall field combining remote sensed data and raingauge observations. Geophysical Research Abstracts, 17, EGU2015-3013. https://meetingorganizer.copernicus.org/EGU2015/EGU2015-3013.pdf, 2015. (Accessed on 06-05-2025).

Polo, M. J., Pimentel, R., Gascoin, S. and Notarnicola, C.: Chapter 3 - Mountain hydrology in the Mediterranean region, Water Resources in the Mediterranean Region, 51-75, Elsevier, doi:10.1016/B978-0-12-818086-0.00003-0, 2020.

Posavec, K., Bačani, A. and Nakić, Z.: A visual basic spreadsheet macro for recession curve analysis, Groundwater, 44(5), 764-767, doi:10.1111/j.1745-6584.2006.00226.x, 2006.

Preziosi, E. Simulazioni Numeriche di Acquiferi Carbonatici in Aree Corrugate: Applicazioni al Sistema Idrogeologico Della Valnerina (Italia Centrale), Quad IRSA-CNR; Istituto di Ricerca Sulle Acque-CNR: Rome, Italy, 125, p. 225, ISSN 0390-6329, 2007.

Preziosi, E., Guyennon, N., Petrangeli, A. B., Romano, E. and Di Salvo, C.: A stepwise modelling approach to identifying structural features that control groundwater flow in a folded carbonate aquifer system, Water, 14(16), 2475, doi:10.3390/w14162475, 2022.

Rateb, A., Scanlon, B. R., Pool, D. R., Sun, A., Zhang, Z., Chen, J., Clark, B., Faunt, C. C., Haugh, C. J., Hill, M., Hobza, C., McGuire, V. L., Reitz, M., Müller Schmied, H., Sutanudjaja, E. H., Swenson, S., Wiese, D., Xia, Y. and Zell, W.: Comparison of groundwater storage changes from GRACE satellites with monitoring and modeling of major US aquifers, Water Resour. Res., 56(12), e2020WR027556, doi:10.1029/2020WR027556, 2020.

Rossi, M., Donnini, M., and Beddini, G.: Nationwide groundwater recharge evaluation for a sustainable water withdrawal over Italy, J. Hydrol. Reg. Stud., 43, 101172, doi:10.1016/j.ejrh.2022.101172, 2022.

Rusi, S. and Di Giovanni, A.: Assessing the Impact of Often Overlooked Snowfall on the Hydrological Balance of Apennine Mountain Aquifers in Central Italy, Water, 17(6), 864, doi:10.3390/w17060864, 2025.

Scanlon, B. R., Healy, R. W. and Cook, P. G.: Choosing appropriate techniques for quantifying groundwater recharge, Hydrogeol. J., 10(1), 18-39, doi:10.1007/s10040-001-0176-2, 2002.

Scanlon, B. R., Fakhreddine, S., Rateb, A., de Graaf, I., Famiglietti, J., Gleeson, T., Grafton,R. Q., Jobbagy, E., Kebede, S., Kolusu, S R., Konikow, L. F., Long, D., Mekonnen, M., Müller Schmied, H., Mukherjee, A., MacDonald, A., Reedy, R. C., Shamsudduha, M., Simmons, C. T., Sun, A., Taylor, R. G., Villholth, K. G., Vörösmarty, C. J. and Zheng, C.: Global water

https://doi.org/10.5194/egusphere-2025-4368
Preprint. Discussion started: 8 October 2025

resources and the role of groundwater in a resilient water future, Nat. rev., Earth environ., 4(2), 87-101, doi:10.1038/s43017-022-00378-6, 2023.

Schaller, M. F. and Fan, Y.: River basins as groundwater exporters and importers: Implications for water cycle and climate modeling, J. Geophys. Res. Atmos., 114(D4), doi:10.1029/2008JD010636, 2009.

Segura, C., Noone, D., Warren, D., Jones, J. A., Tenny, J., and Ganio, L. M.: Climate, landforms, and geology affect baseflow sources in a mountain catchment, Water Resour. Res., 55(7), 5238-5254, doi:10.1029/2018WR023551, 2019.

Shakti, P. C. and Sawazaki, K.: River discharge prediction for ungauged mountainous river basins during heavy rain events based on seismic noise data, PEPS, 8(1), 58, doi:10.1186/s40645-021-00448-1, 2021.

Singh, V. P. and Woolhiser, D. A.: Mathematical modeling of watershed hydrology, J. Hydrol. Eng., 7(4), 270-292, doi:10.1061/(ASCE)1084-0699(2002)7:4(270), 2002.

Skamarock, W. C., Klemp, J. B., Dudhia, J., Gill, D. O., Barker, D. M., Duda, M. G., Huang, X.-Y., Wang, W., Powers, J. G.,: A description of the advanced research WRF Version 3, NCAR tech. note ncar/tn-475+str, doi:10.5065/D68S4MVH, 2008.

Smakhtin, V. U.: Low flow hydrology: a review, J. Hydrol., 240(3-4), 147-186, doi:10.1016/S0022-1694(00)00340-1, 2001.

Somers, L. D. and McKenzie, J. M.: A review of groundwater in high mountain environments, WIREs Water, 7(6), e1475, doi:10.1002/wat2.1475, 2020.

Sprenger, M., Leistert, H., Gimbel, K. and Weiler, M.: Illuminating hydrological processes at the soil-vegetation-atmosphere interface with water stable isotopes, Rev. Geophys., 54(3), 674-704, doi:10.1002/2015RG000515, 2016.

Tallaksen, L. M.: A review of baseflow recession analysis, J. Hydrol., 165(1-4), 349-370, doi:10.1016/0022-1694(94)02540-R,1995.

Tan, S. B., Lo, E. Y. M., Shuy, E. B., Chua, L. H. and Lim, W. H.: Hydrograph separation and development of empirical relationships using single-parameter digital filters, J. Hydrol. Eng., 14(3), 271-279, doi:10.1061/(ASCE)1084-0699(2009)14:3(271), 2009.

Tarragoni, C.: Determinazione della “quota isotopica” del bacino di alimentazione delle principali sorgenti dell’alta Valnerina, Geologica Romana, 39, 55-62, 2006.

Tazioli, A., Fronzi, D. and Palpacelli, S.: Regional vs. Local Isotopic Gradient: Insights and Modeling from Mid-Mountain Areas in Central Italy, Groundwater, 62(5), 714-734, doi:10.1111/gwat.13395, 2024.

Thornthwaite, C. W. and Mather, J. R.: The Water Balance, Laboratory in Climatology, Johns Hopkins University: Baltimore, MD, USA, 8,1–104, 1955.

Thornthwaite, C. W. and Mather, J. R.: Instructions and Tables for Computing Potential Evapotranspiration and the Water Balance, Laboratory in Climatology, Johns Hopkins University: Baltimore, MD, USA, 10, 181–311, 1957.

Tipper, E. T., Bickle, M. J., Galy, A., West, A. J., Pomiès, C. and Chapman, H. J: The short term climatic sensitivity of carbonate and silicate weathering fluxes: insight from seasonal variations in river chemistry, Geochimica et Cosmochimica Acta, 70(11), 2737-2754, doi:10.1016/j.gca.2006.03.005, 2006.

https://doi.org/10.5194/egusphere-2025-4368
Preprint. Discussion started: 8 October 2025

Uboldi, F., Lussana, C. and Salvati, M.: Three-dimensional spatial interpolation of surface meteorological observations from high-resolution local networks, Meteorological Applications: A journal of forecasting, practical applications, training techniques and modelling, 15(3), 331-345, doi:10.1002/met.76, 2008.

Valigi, D., Cambi, C., Checcucci, R. and Di Matteo, L.: Transmissivity estimates by specific capacity data of some fractured Italian carbonate aquifers, Water, 13, 1374, doi:10.3390/w13101374, 2021.

Viaroli, S., Mastrorillo, L., Lotti, F., Paolucci, V. and Mazza, R.: The groundwater budget: a tool for preliminary estimation of the hydraulic connection between neighboring aquifers, J. Hydrol., 556, 72-86, doi:10.1016/j.jhydrol.2017.10.066, 2018.

White, J. C., Khamis, K., Dugdale, S., Jackson, F. L., Malcolm, I. A., Krause, S., and Hannah, D. M.: Drought impacts on river water temperature: A process-based understanding from temperate climates, Hydrol. Process., 37(10), e14958, doi:10.1002/hyp.14958, 2023.

Winter, T. C.: The concept of hydrologic landscapes 1, JAWRA, 37(2), 335-349, doi:10.1111/j.1752-1688.2001.tb00973.x, 2001.

World Meteorological Organization (WMO): Guide to Meteorological Instruments and Methods of Observation: (CIMO Guide), WMO-No. 8. Geneva: World Meteorological Organization, http://hdl.handle.net/11329/365, 2014.

Xanke, J., Goldscheider, N., Bakalowicz, M., Barberá, J. A., Broda, S., Chen, Z., Ghanmi, M., Günther, A., Hartmann, A., Jourde, H., Liesch, T., Mudarra, M., Petitta, M., Ravbar, N. and Stevanović, Z.: Carbonate rocks and karst water resources in the Mediterranean region, Hydrogeol. J., 32(5), 1397-1418, doi:10.1007/s10040-024-02810-1, 2024.

Yin, W., Zhang, G., Han, S. C., Yeo, I. Y. and Zhang, M.: Improving the resolution of GRACE-based water storage estimates based on machine learning downscaling schemes, J. Hydrol., 613, 128447, doi:10.1016/j.jhydrol.2022.128447, 2022.

Zheng, X., Liu, D., Huang, S., Wang, H. and Meng, X.: Achieving water budget closure through physical hydrological processes modelling: insights from a large-sample study, HESSD, 1-36, doi:10.5194/hess-29-627-2025, 2025.